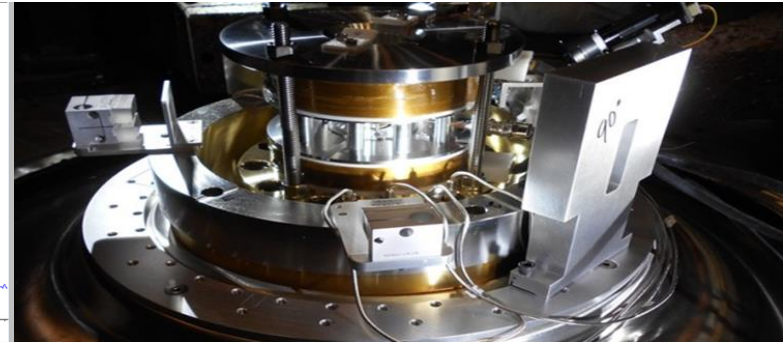
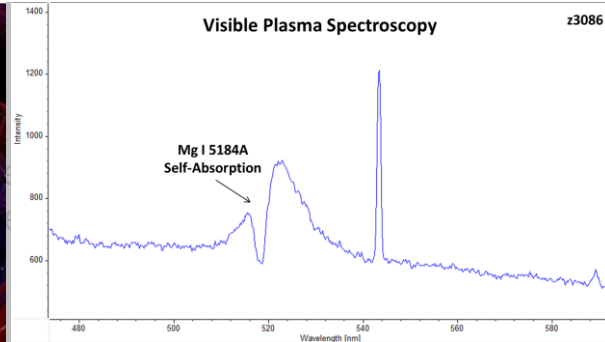
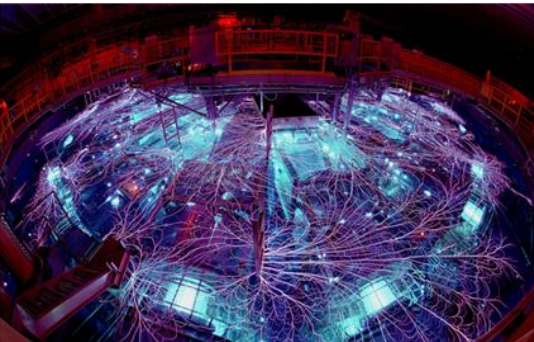


Exceptional service in the national interest



Spectroscopy Techniques for Diagnosing Plasmas in High Energy Density, Pulsed-Power Accelerators

M.D. Johnston¹, S.G. Patel¹, M.L. Kiefer¹, M.E. Cuneo¹, E. Stambulchik²,
R. Doron², and Y. Maron²

¹Sandia National Laboratories, Albuquerque, NM 87185, USA

²Weizmann Institute of Science, Rehovot, Israel



Sandia National Laboratories is a multimission laboratory managed and operated by National Technology and Engineering Solutions of Sandia, LLC, a wholly owned subsidiary of Honeywell International, Inc., for the U.S. Department of Energy's National Nuclear Security Administration under contract DE-NA0003525.

Abstract

Pulsed power devices rely on the ability to deliver high voltages and currents to a variety of complex loads with minimal transmission losses. The Z Machine at Sandia National Laboratories can deliver up to 26MA within ~100 nanoseconds to multiple physics targets. This type of current flow combined with MeV potentials across millimeter A-K vacuum gaps lead to a variety of extreme electrode heating conditions, which liberate both surface and entrained gases, forming plasmas that propagate into the vacuum gap and draw current from the load. Losses of up to 20% have been observed on Z for certain load configurations. An effort is underway to investigate plasma generation in the power flow regions of the Z Machine. Visible plasma spectroscopy is employed to spatially and temporally determine plasma formation and propagation, and to measure plasma parameters such as densities and temperatures. In addition to plasma parameters, measurements of magnetic and electric fields by Zeeman splitting and Stark shifts, respectively, are also conducted [1]. Measurements are made using multifiber arrays, input into streak and fast-gated spectrometers. Line shape analyses are performed using detailed, time-dependent, collisional-radiative (CR) and radiation transport modeling. Recent results will be discussed.

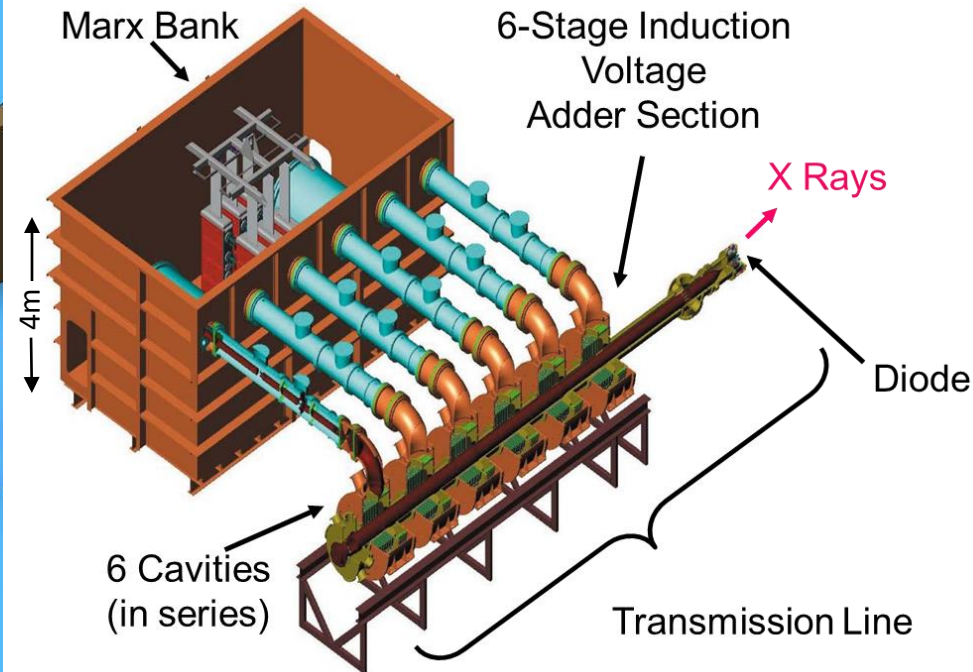
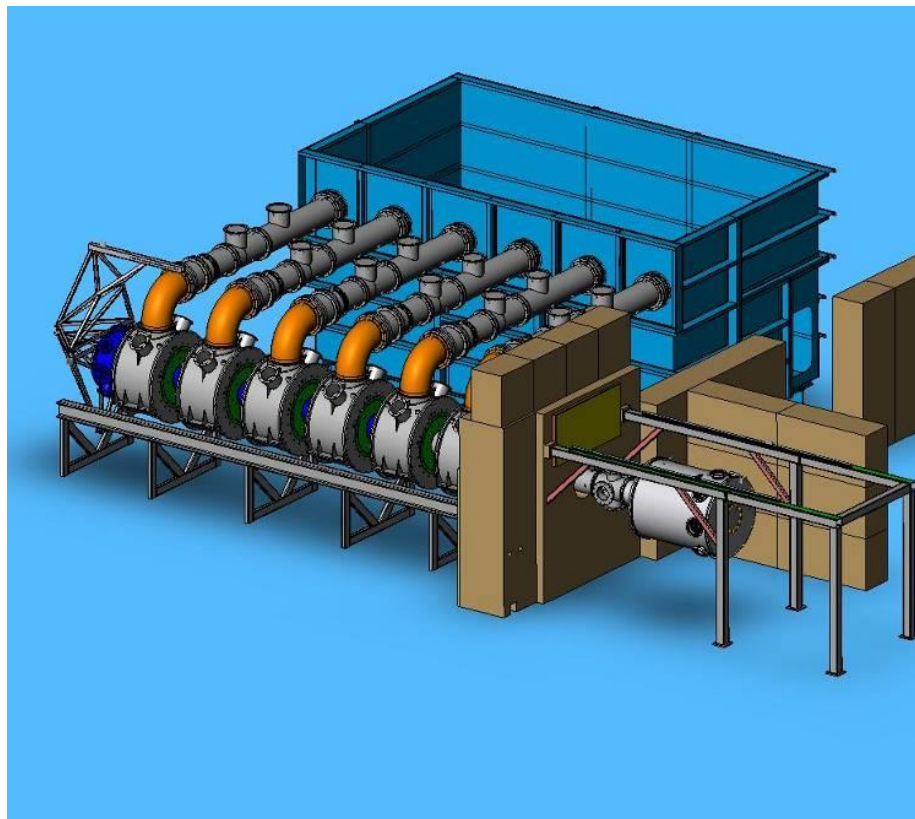
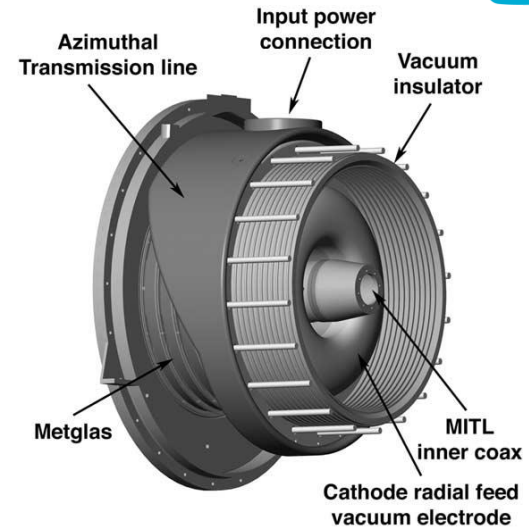
[1] S. Biswas, M.D. Johnston, et. al., “Shielding of the Azimuthal Magnetic Field by the Anode Plasma in a Relativistic Self-Magnetic-Pinch Diode,” *Physics of Plasmas*, 25, 113102 (2018).

Outline

- **RITS-6 Accelerator at Sandia National Laboratories (SNL)**
- **Self-Magnetic Pinch (SMP) E-beam Diode**
- **Plasma Diagnostics Fielded at RITS**
- **Zeeman Splitting Measurements (B-field)**
- **Stark Shift Measurements (E-field)**
- **Summary of RITS Work**
- **Z-Machine**
- **Power Flow Studies on Z**
- **Current Loss Mechanisms**
- **Initial Experimental Results**
- **Zeeman Measurements with Hydrogen**
- **Zeeman and Stark Measurements with Lithium**
- **Other Experimental Platforms on Z**
- **Summary and Conclusions**
- **Z-Next**
- **Future Work**

RITS-6 Pulsed-Power Accelerator at Sandia National Laboratories (SNL)

RITS-6 is a 8-11 MeV Marx driven six-stage Inductive Voltage Adder (IVA) capable of driving a variety of electron beam diodes [2].



Inductive Voltage Adders

Each pulser operates as a primary to a common secondary
high voltage only appears as a coaxial vacuum transmission line wave

Injected pulse $V = IR$

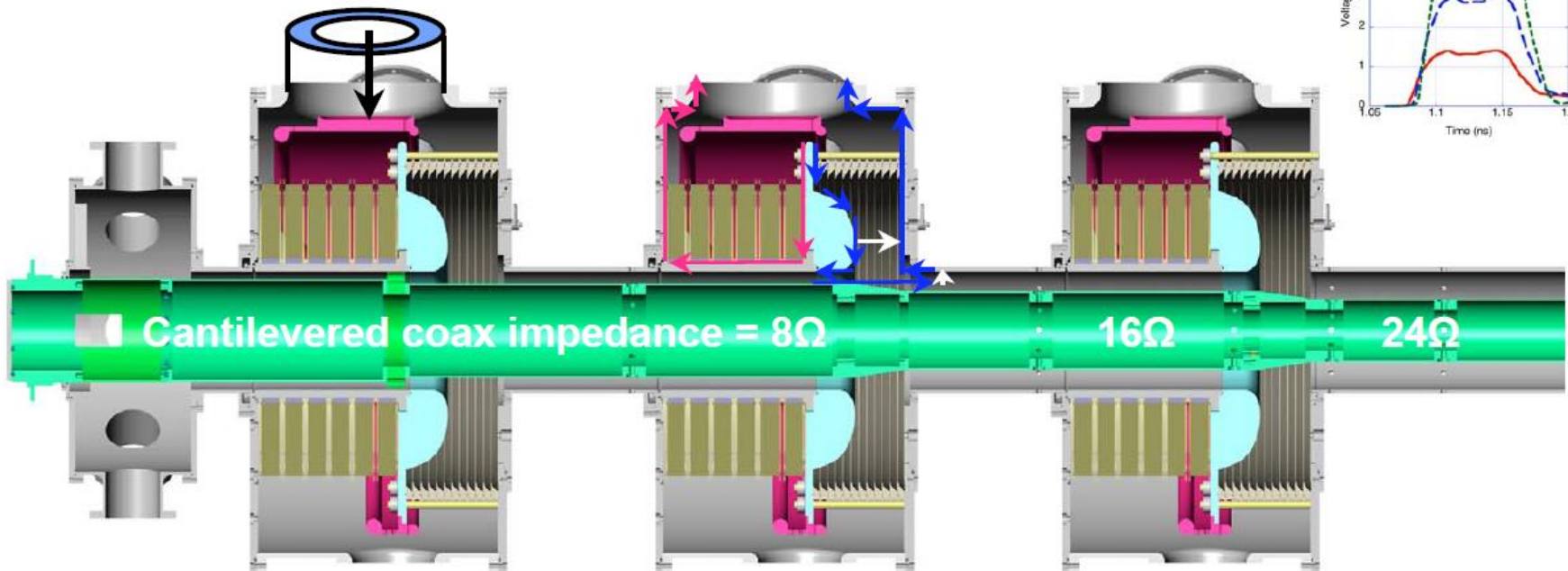
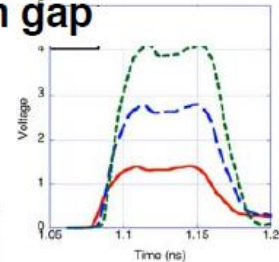
$$1.3 \text{ MV} = 160 \text{ kA} * 8 \Omega$$

Currents split

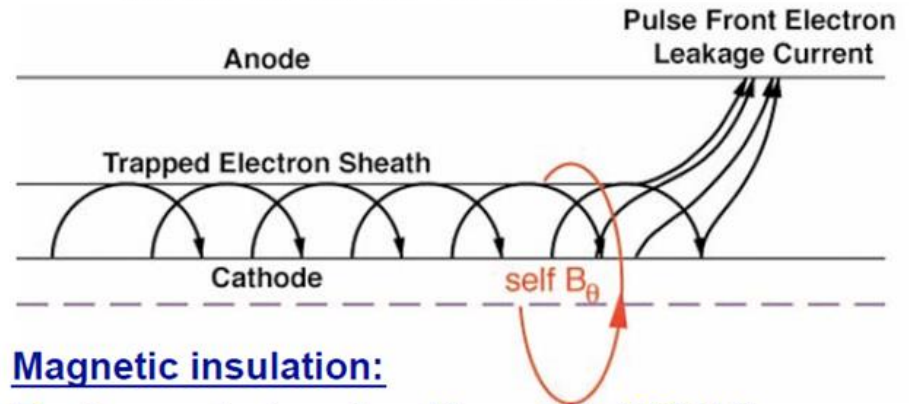
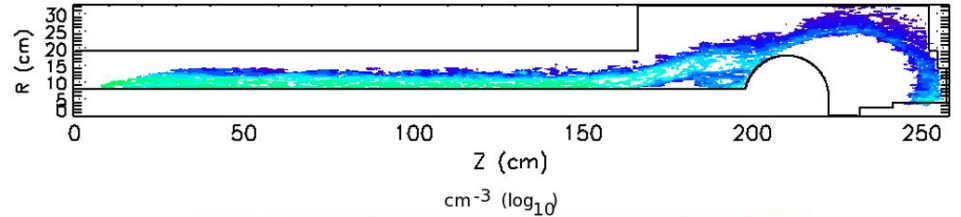
$$I = I_{\text{left}} + I_{\text{right}}$$

$$160 \text{ kA} = 5 \text{ kA} + 155 \text{ kA}$$

Voltage ($V = IR$)
across vacuum gap



Magnetically Insulated Transmission Lines



Magnetic insulation:

Electron emission when V exceeds 250 kV/cm

Efficient sheath flow when $a_L <$ radial gap

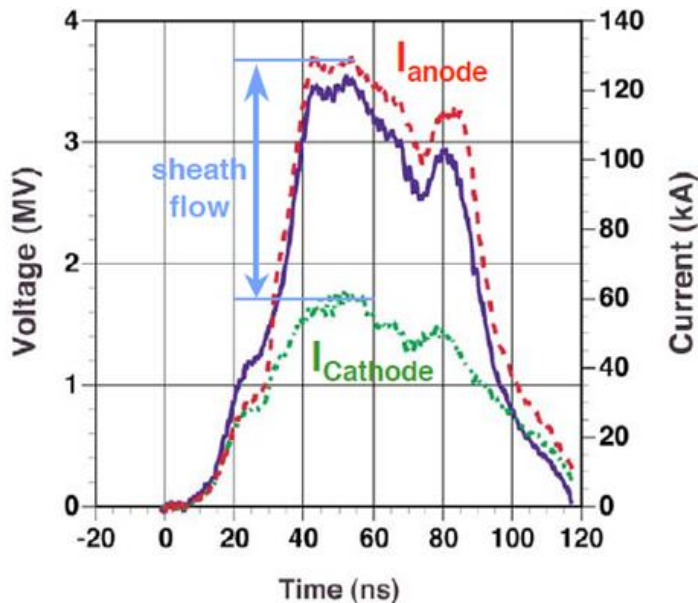
Wave travels at $\sim 0.8c$

MITL self-limits to an overmatched load - no voltage gain

Voltage is calculable from the currents

$$V_{MITL} = Z_0(I_a^2 - I_c^2)^{1/2} - (60mc^2/e)(I_a/I_c - 1)[\alpha(2(I_a/I_c + 1)^{1/2} - 1)]$$

High-Z MITL mismatches the drive to create higher voltage and less current in the IVA adder.



Self-Magnetic Pinch Diode (SMP)

Cathode: Aluminum, hollowed cylinder (12.5mm OD, 8.5mm ID) with 25.4mm long silver suspension on tip for enhanced electron turn-on.

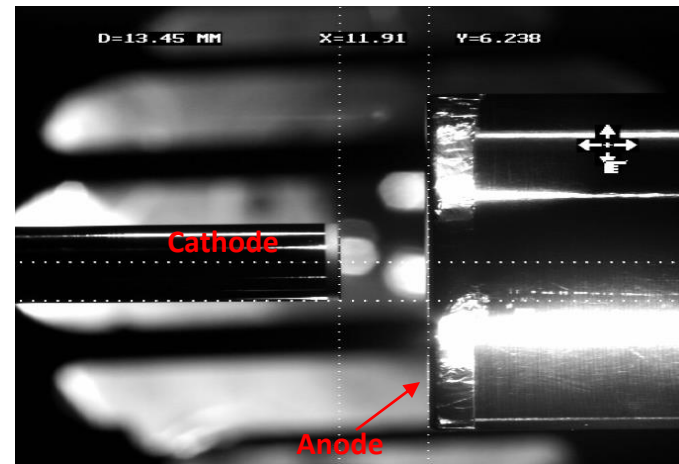
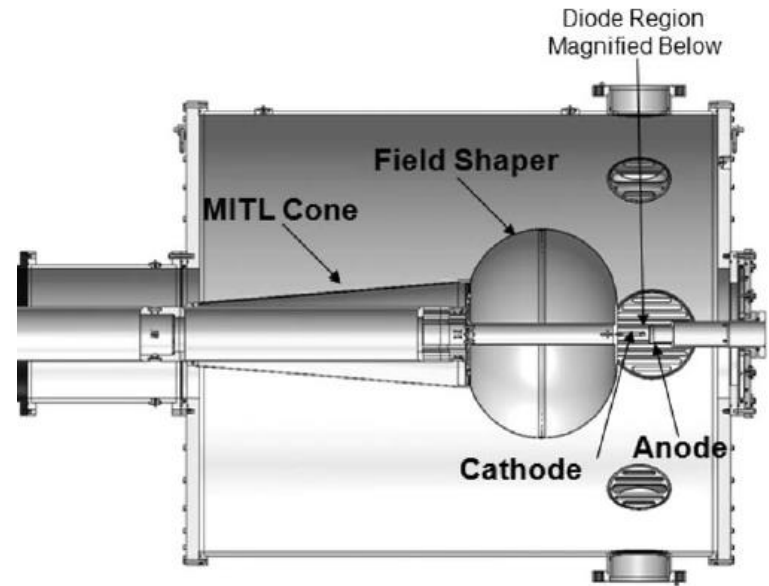
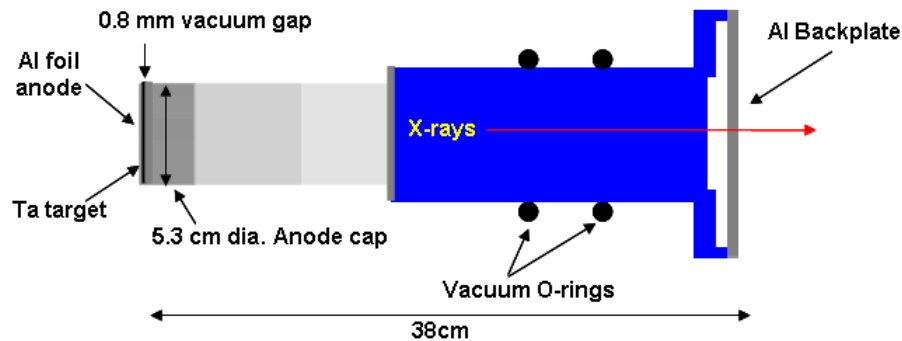
Anode: Aluminum foil (10 μ m)

Target: 1/3 range thick tantalum (1.0mm). Positioned 0.8mm behind the aluminum foil.

A-K Gap: 12.0mm (standard setup)

Aspect ratio (D/d): 1.0

Beamstops: 2 aluminum plates with a total thickness of 14mm

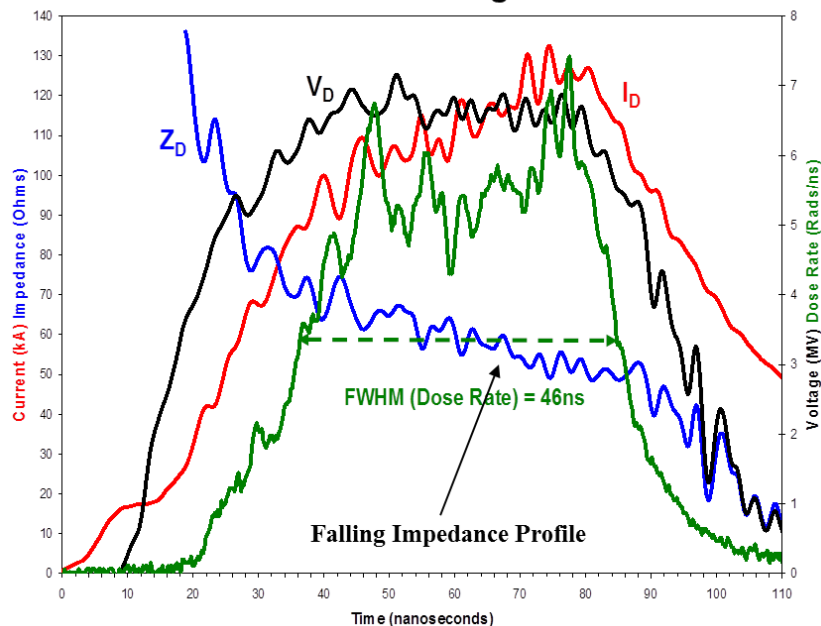


Alignment Camera Image

+/- 100 μ m accuracy

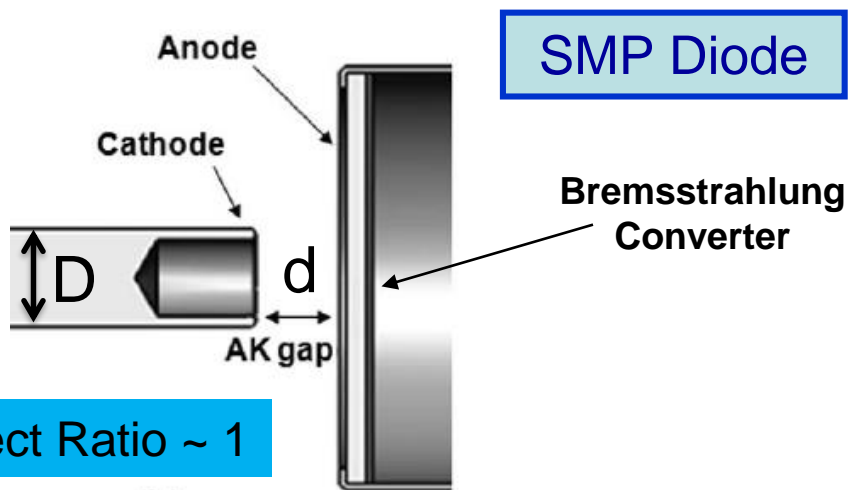
Characteristics of the SMP Diode as Fielded on the RITS-6 Accelerator

Current and Voltage Profiles

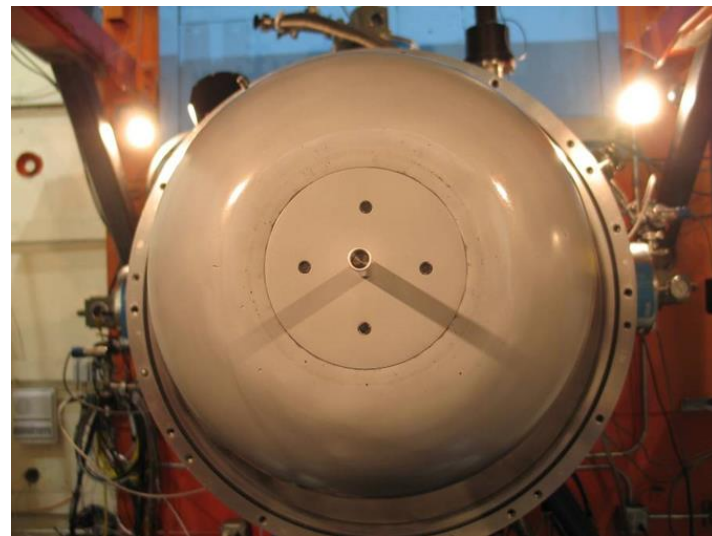


SMP Diode Parameters [3]

- 6-8.5 MV
- 150 kA (~15% ions)
- 50 Ω Impedance
- 70ns Electrical Pulse
- 45ns Radiation Pulse
- > 350 Rads @ 1 meter
- < 3 mm focal spot size



Aspect Ratio ~ 1

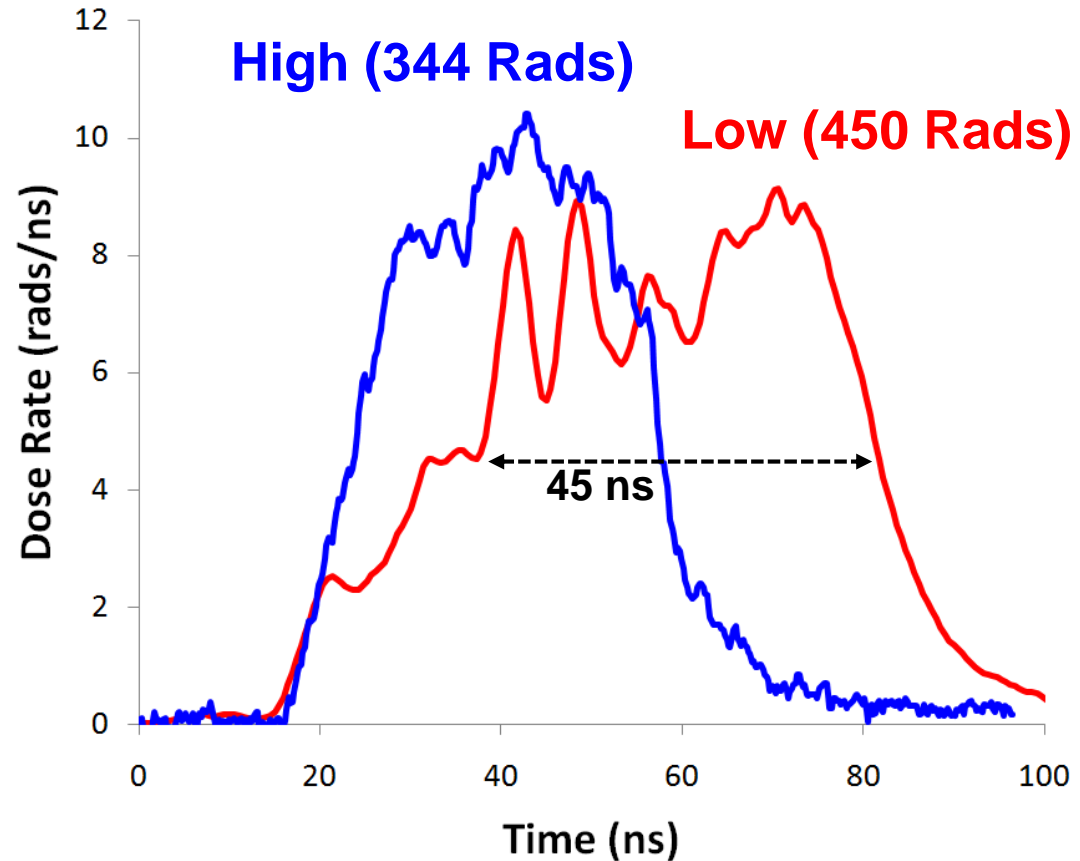


Comparison of High and Low Impedance MITLs on RITS-6

Low impedance **High impedance**

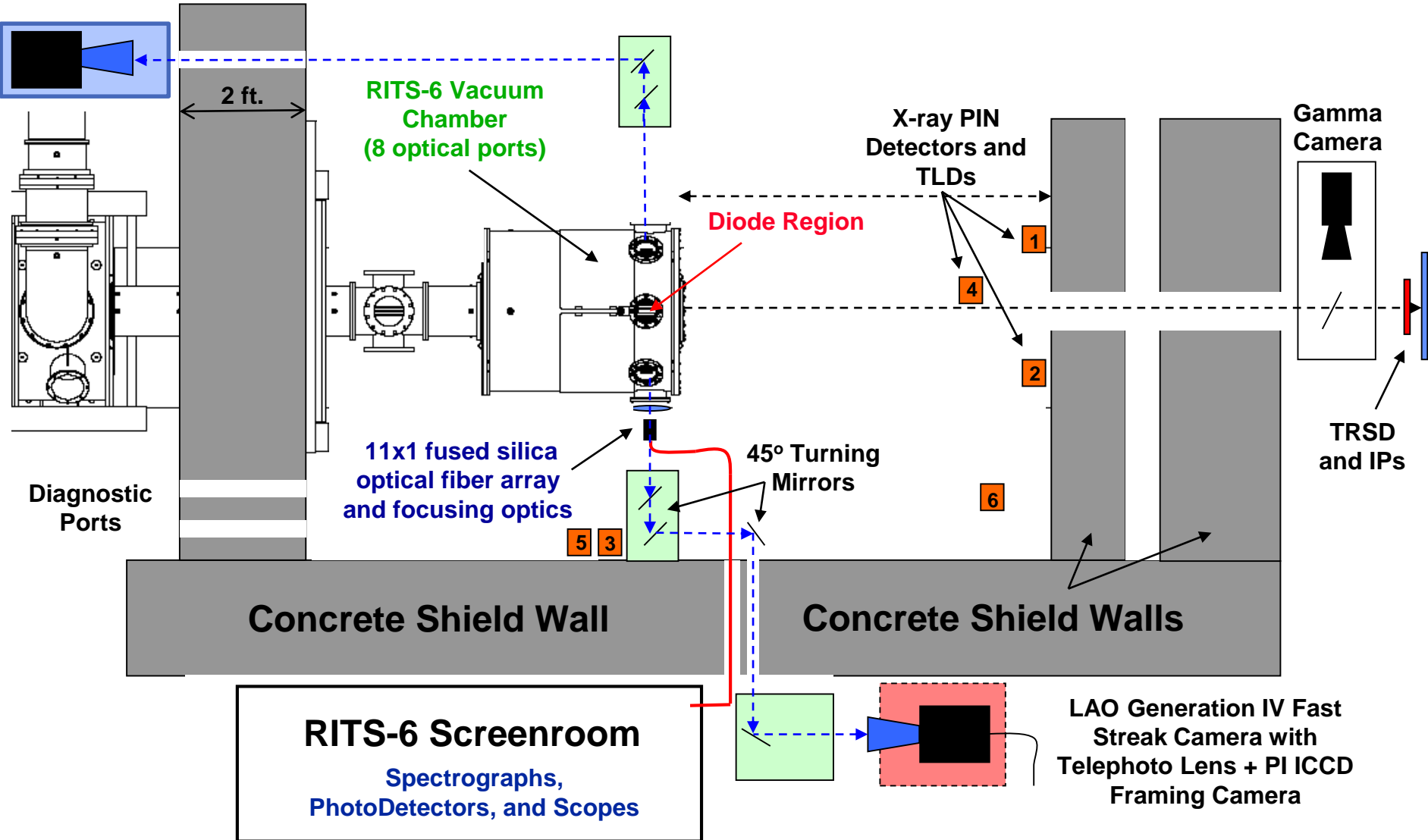
| | | |
|-----------------------------|---------------|--|
| Accelerator Impedance | ~ 40 Ω | ~ 80 Ω <i>same as Merlin</i> |
| Diode Impedance | ~ 50 Ω | ~ 50 Ω |
| Peak Accelerator Voltage | 8.5 MV | 11.5 MV |
| Peak Diode Voltage | 8 MV | 8.5 MV |
| Electrical pulse width FWHM | 70 ns | 70 ns |
| X-ray pulse width FWHM | 45 ns | 35 ns |

Radiation Output

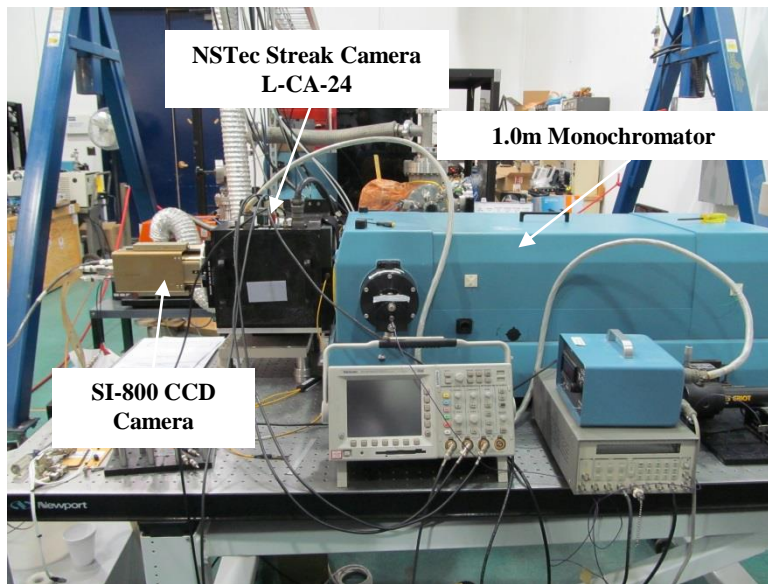
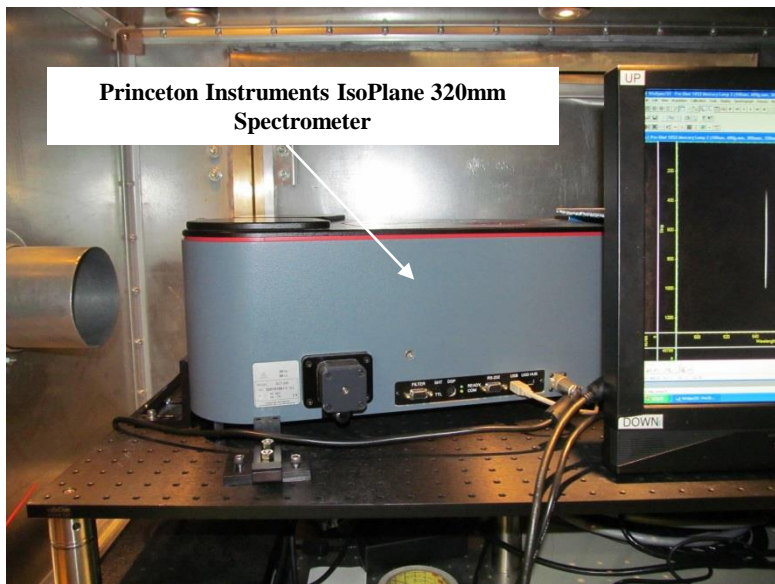
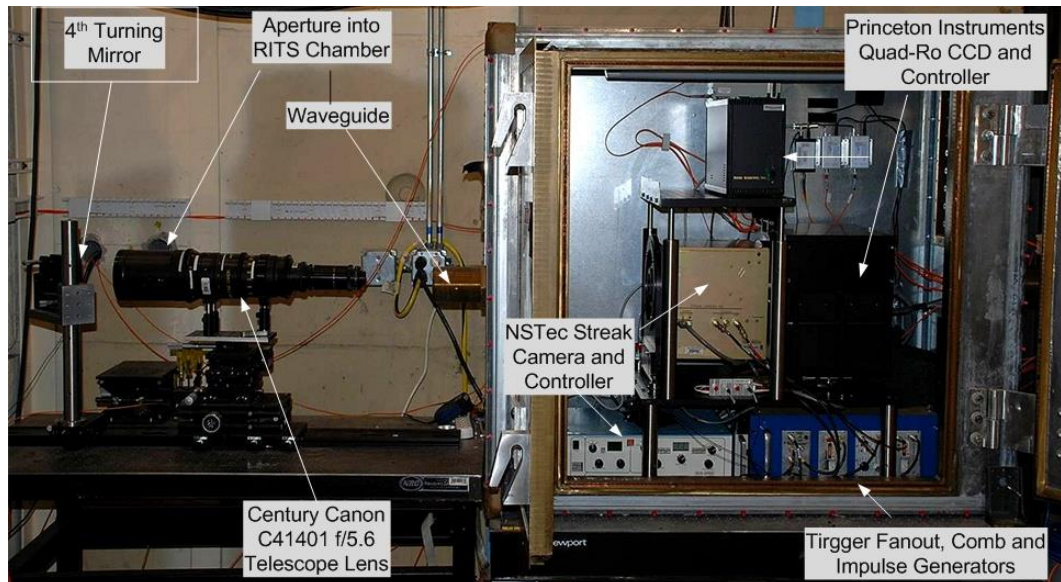
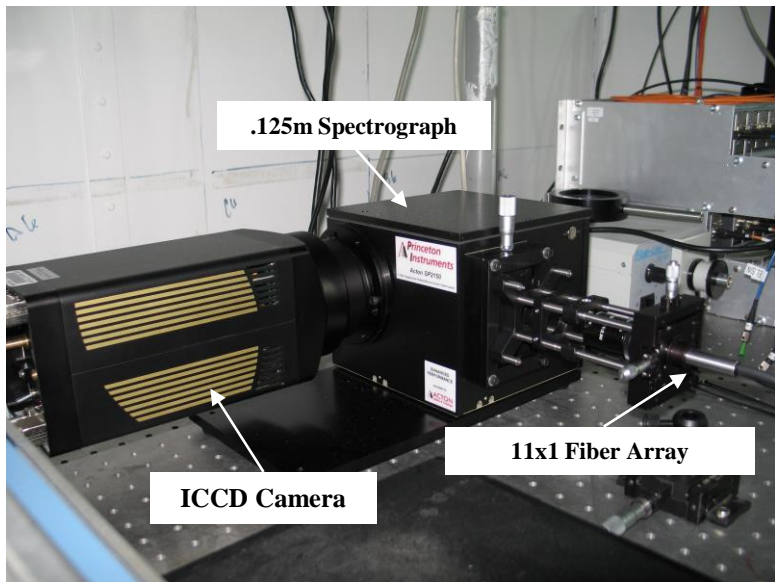


Diagnostic Layout around the RITS-6 Accelerator

Ultra8 Multiframe Imaging Camera or Direct Imaging Spectroscopy



Imaging and Spectral Diagnostics on RITS-6



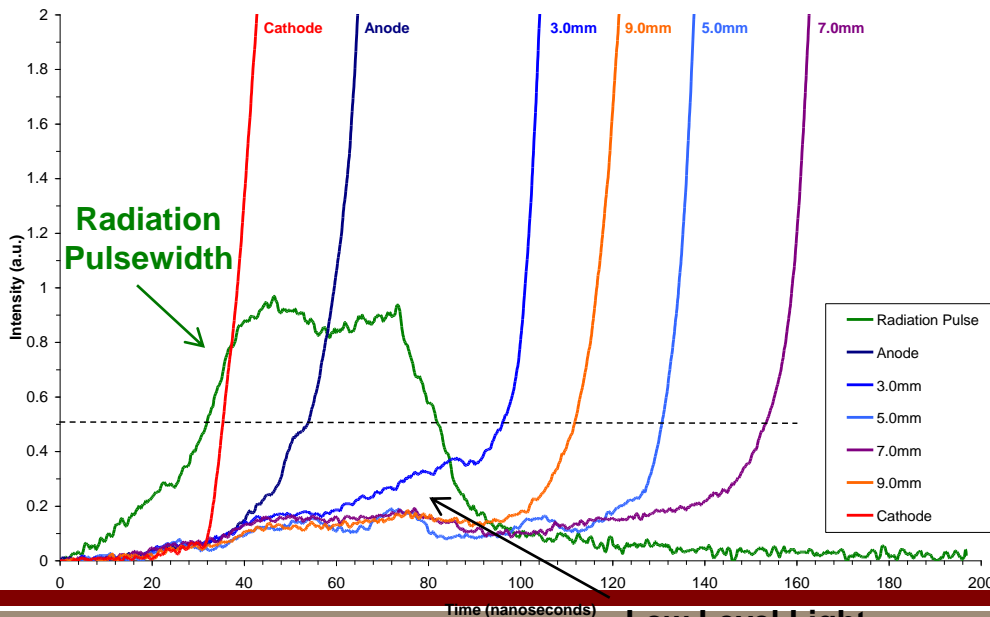
Plasma Measurements using Silicon Avalanche Photodiodes



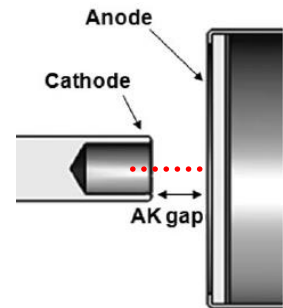
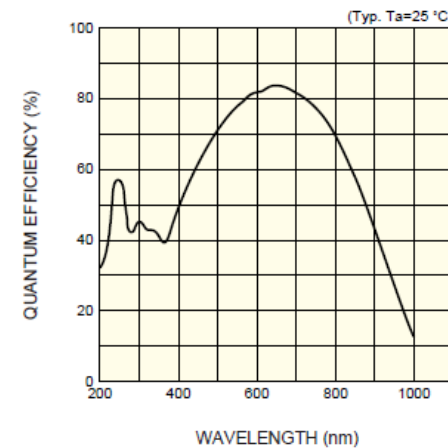
NSTec Model H-EO-53 Avalanche Photodiode

- Hamamatsu Model S5343 Silicon Photodiode
- Bandwidth: 180MHz
- Optical Input Power: 1-100 μW
- Output Impedance: 50 Ohms
- Responsivity: 0.33-20 kV/W
- Linearity: +/- 5%
- Error: +/- 10% (between 8-100 μW)
- Scaling Ratio: 1mV/ μW
- Wavelength Range: 200-1000nm
- Gain (M): 1-50x
- Quantum Efficiency: 80% @ 620nm
- Photosensitivity: 0.42 A/W @620nm (M=1)

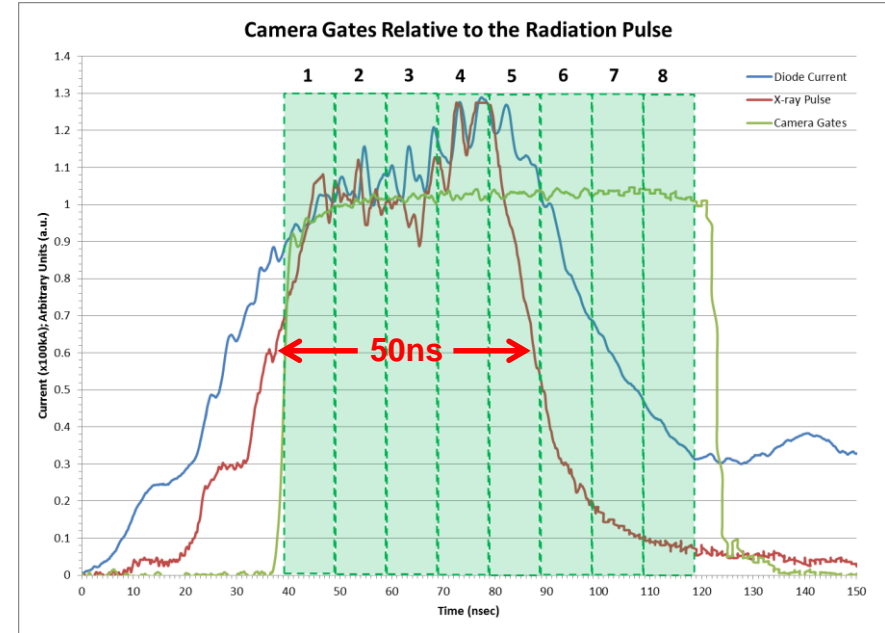
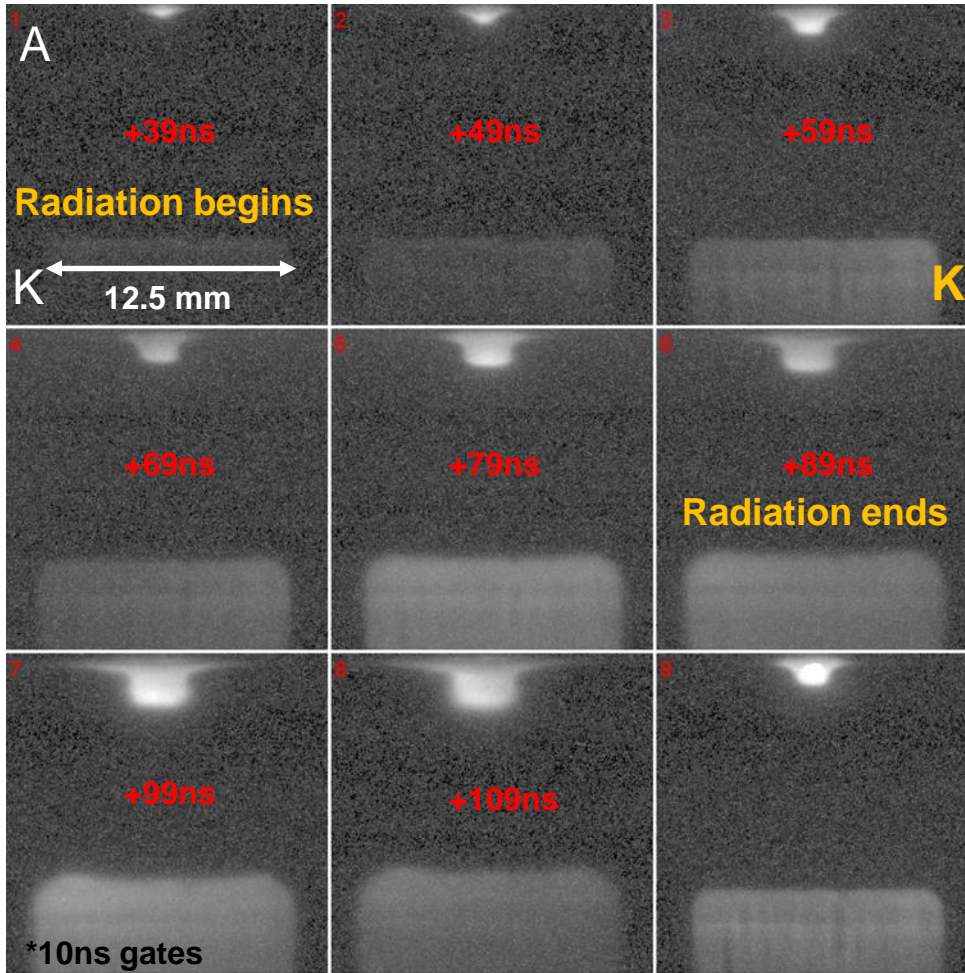
Anode Expansion Velocity: 4.8-8.7cm/ μsec
Cathode Expansion Velocity: 2.6-4.8cm/ μsec



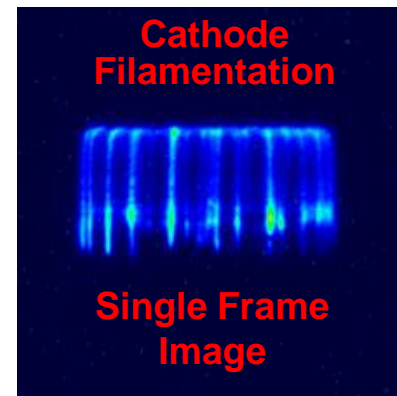
Low Level Light Emission



Self-Emission Images Reveal Structure and Apparent Closure Velocities of Diode Plasmas



FWHM of Radiation Pulse: 50ns



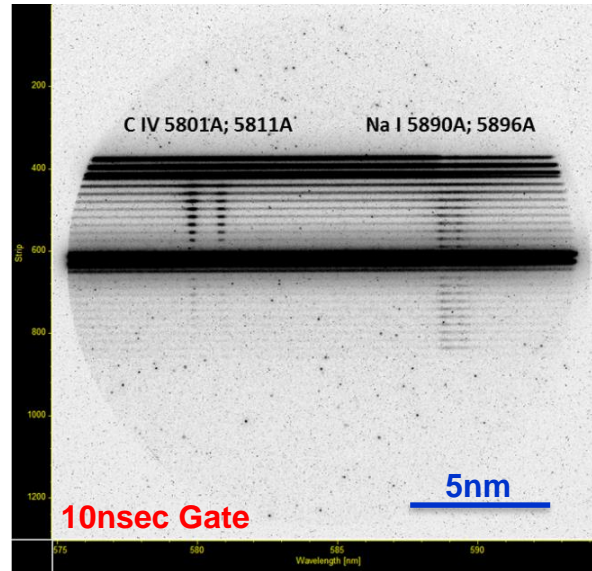
Filament formation on cathode could drive:

- Non-uniform anode plasma
- Field fluctuations
- Thermal instability

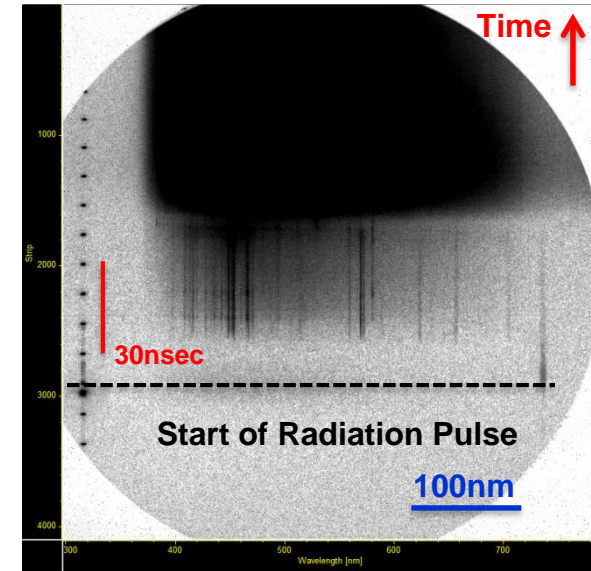
- Need similar diagnostics on Z.

Plasma Measurements Taken on the SMP Diode

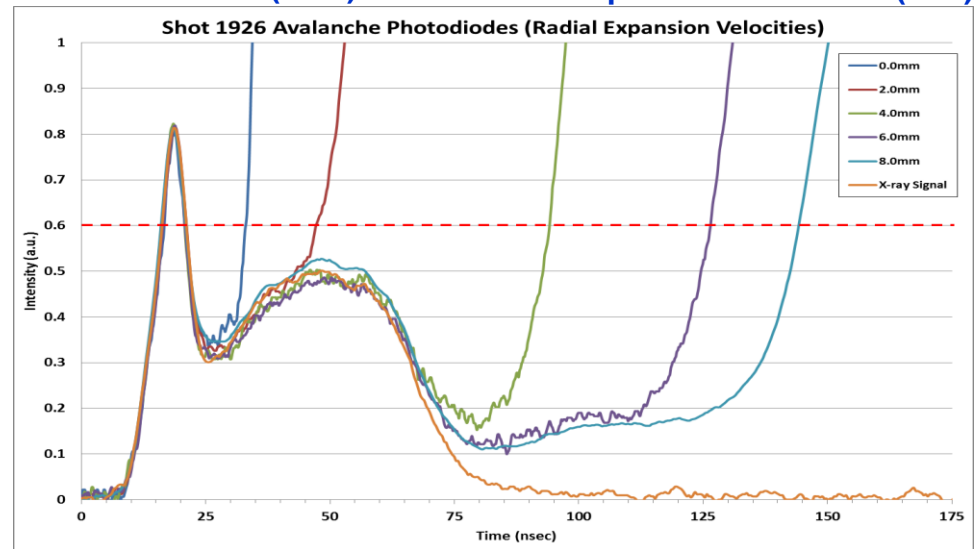
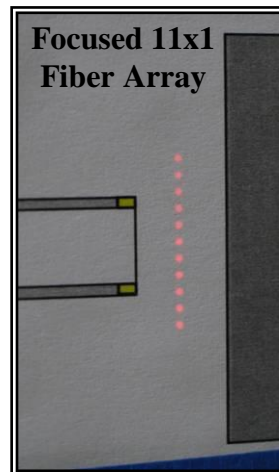
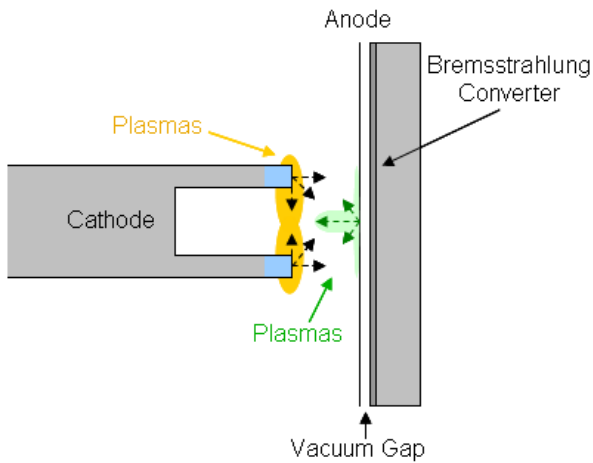
- Multi-Fiber Gated spectra
- Streaked spectra
- Avalanche Photodiodes



High Spectral Resolution (0.5Å)



Lower Spectral Resolution (10Å)



Sample Analyses of Spectral Data off the Anode Surface Following the Radiation Pulse

Fiber 6 (4.0mm off-axis on the anode surface)

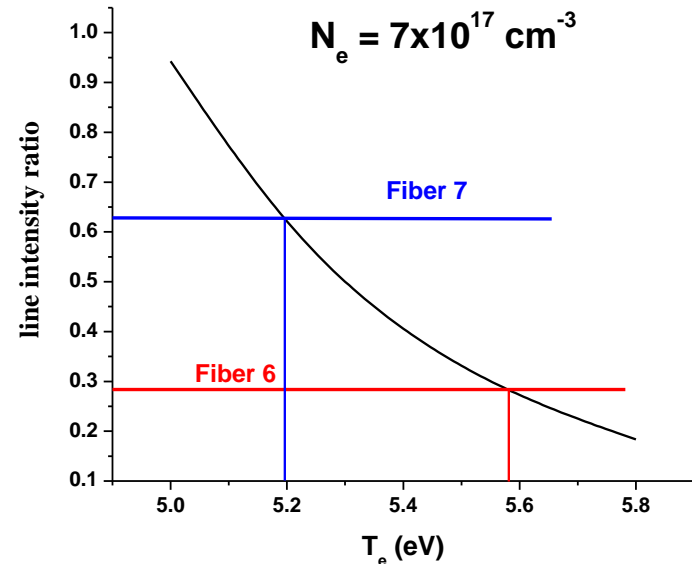
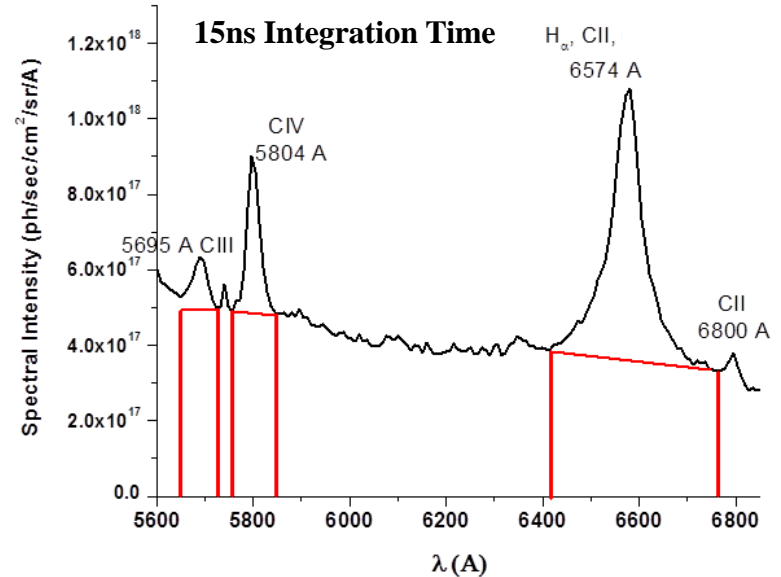
| | | |
|---------------------------------|--------------------------------------|--------------|
| N_e from H-alpha: | $1.1 \times 10^{18} \text{ cm}^{-3}$ | |
| N_e from Continuum: | $6.1 \times 10^{17} \text{ cm}^{-3}$ | |
| Electron Temp. (T_e): | 5.6eV | |
| $N_{\text{hydrogen}} (Z = 1)$: | $3.2 \times 10^{17} \text{ cm}^{-3}$ | (28%) |
| $N_{\text{carbon}} (Z = 2.9)$: | $4.0 \times 10^{16} \text{ cm}^{-3}$ | (10%) |
| $N_{e(\text{oxygen and Al})}$: | $7.0 \times 10^{17} \text{ cm}^{-3}$ | (62%) |

Fiber 7 (6.0mm off-axis on the anode surface)

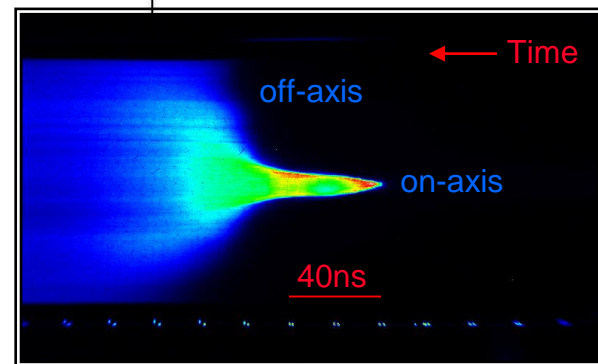
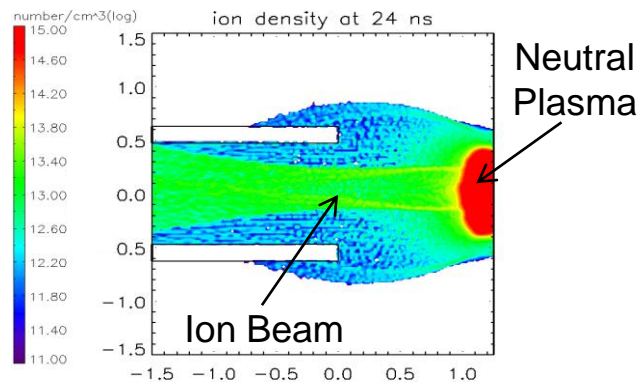
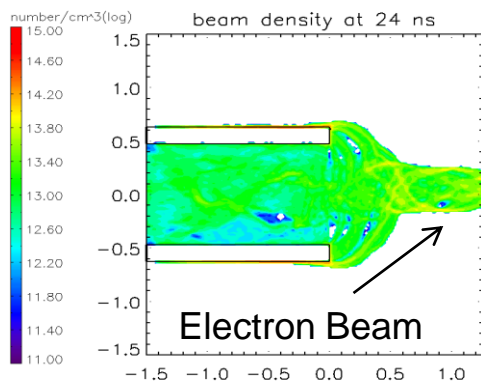
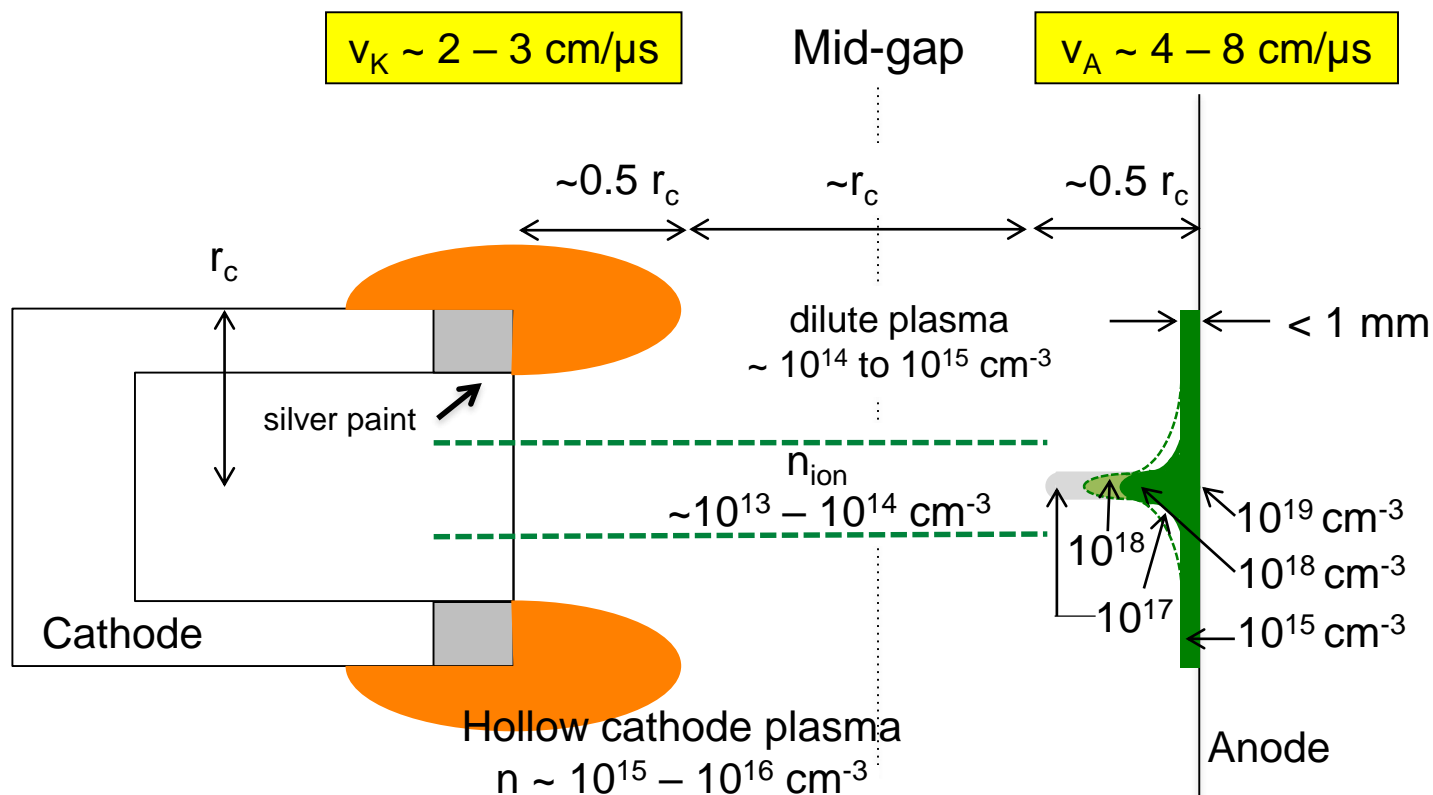
| | | |
|---------------------------------|--------------------------------------|--------------|
| N_e from H-alpha: | $7.4 \times 10^{17} \text{ cm}^{-3}$ | |
| N_e from Continuum: | $2.9 \times 10^{17} \text{ cm}^{-3}$ | |
| Electron Temp. (T_e): | 5.2eV | |
| $N_{\text{hydrogen}} (Z = 1)$: | $3.2 \times 10^{17} \text{ cm}^{-3}$ | (45%) |
| $N_{\text{carbon}} (Z = 2.9)$: | $3.0 \times 10^{16} \text{ cm}^{-3}$ | (12%) |
| $N_{e(\text{oxygen and Al})}$: | $3.0 \times 10^{17} \text{ cm}^{-3}$ | (43%) |

*Continuum density is averaged over the full fiber viewing area, while Stark broadening is a localized measurement.

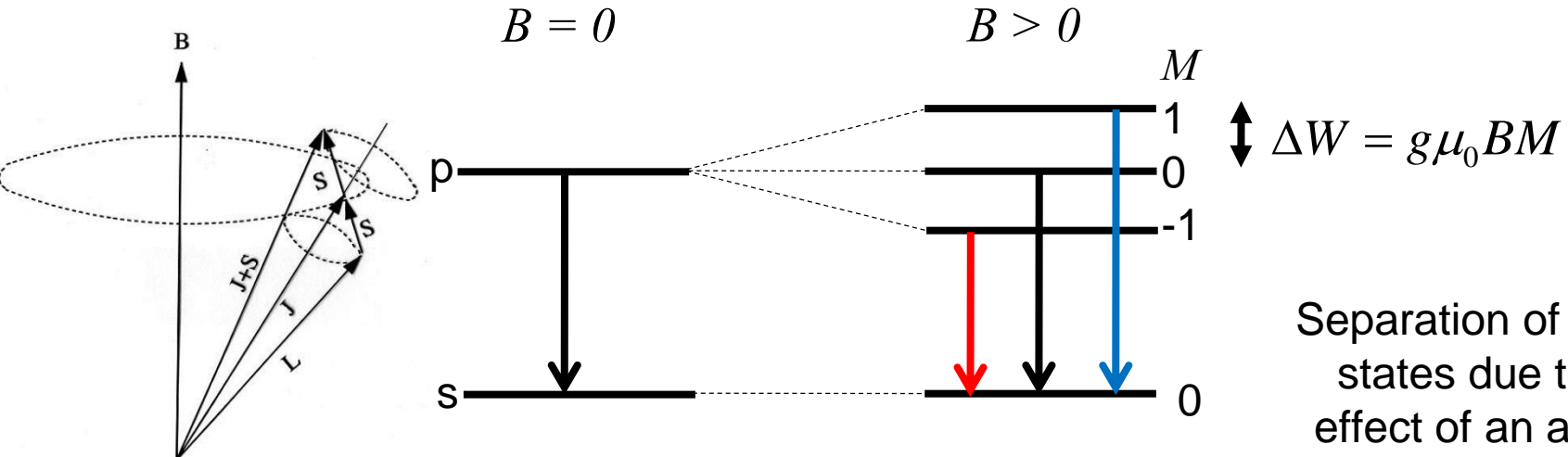
**Analyses use the optical streak images to determine pathlengths through the plasma volumes in time.



Plasma Dynamics within the SMP Diode

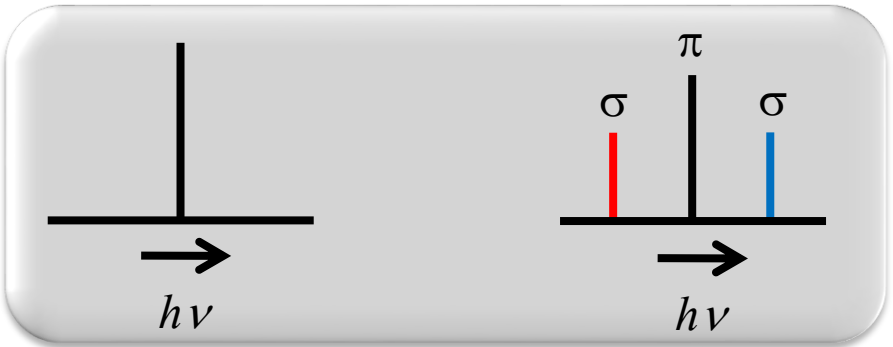


Zeeman Splitting is a Useful Technique for Magnetic Field Measurements in Plasmas



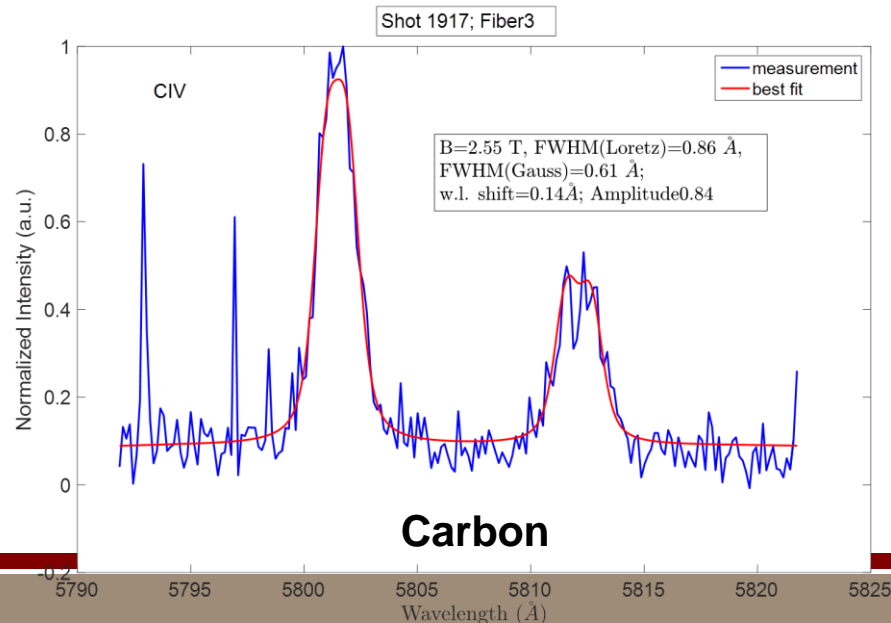
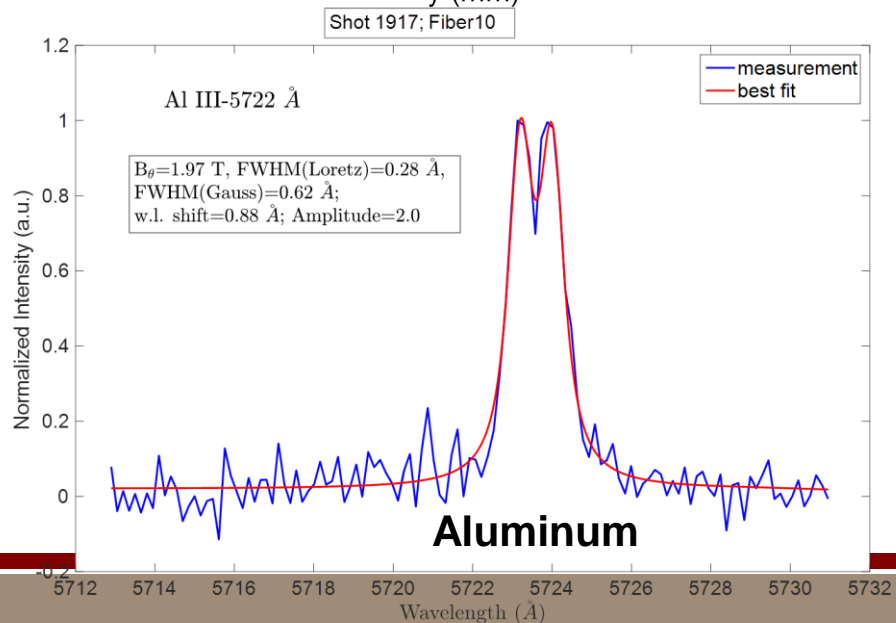
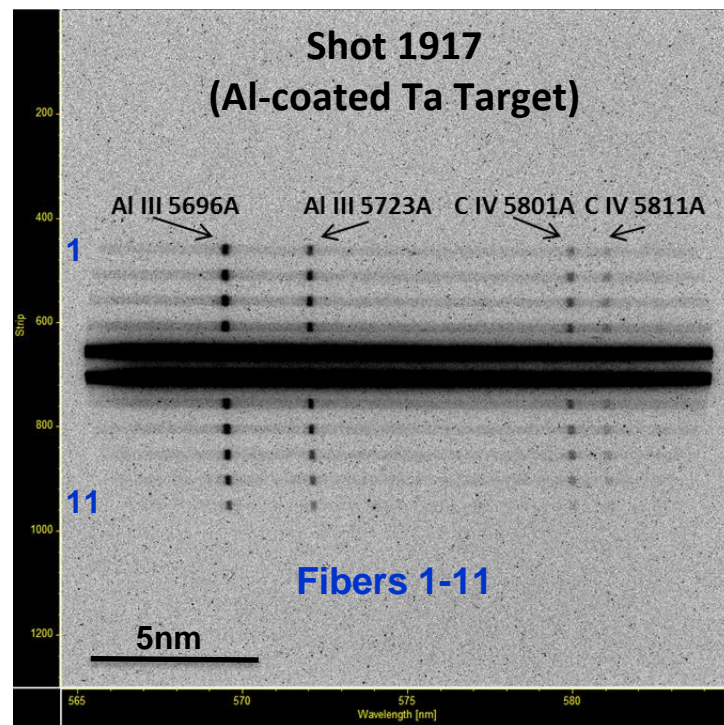
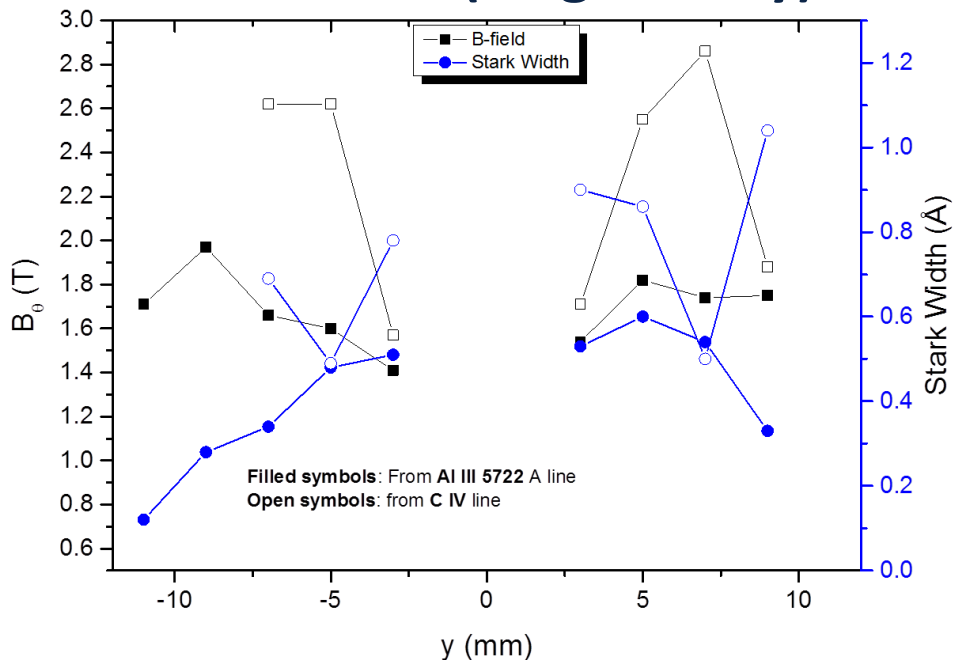
Separation of energy states due to the effect of an applied B-field on the magnetic moment of an atom or ion.

Observed

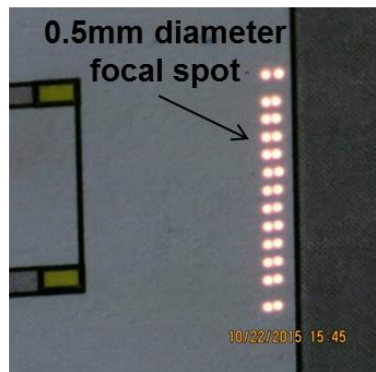
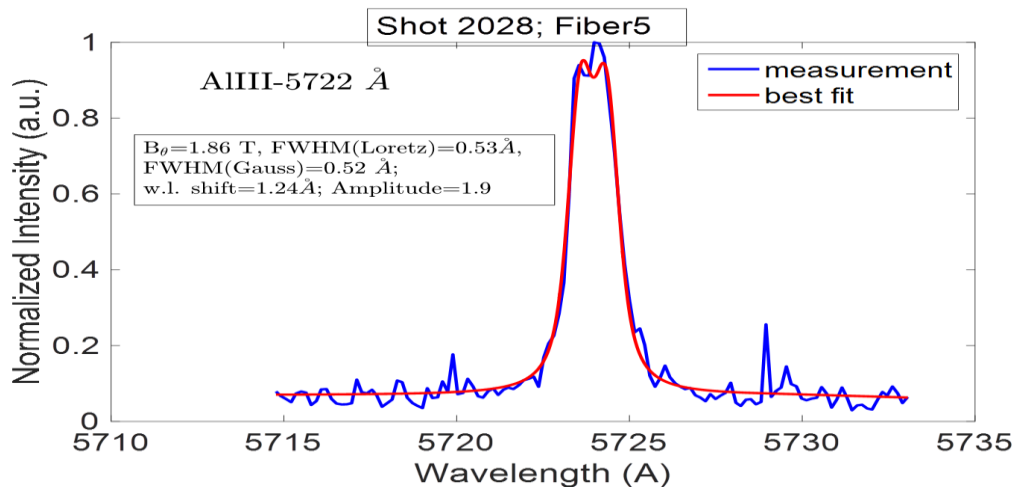
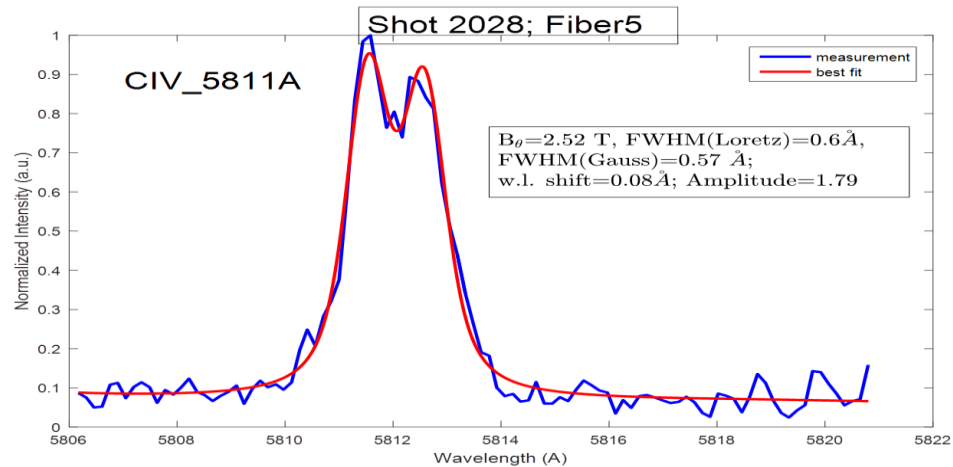
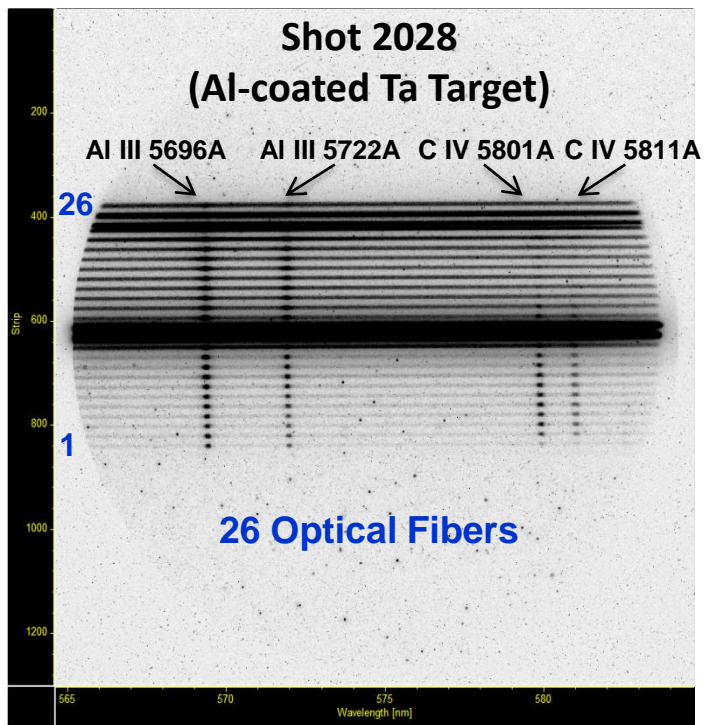


$$h\Delta\nu = \mu_0 B (g_u M_u - g_l M_l), \quad \left[\begin{array}{l} \Delta M = 0, \pi \\ \Delta M = \pm 1, \sigma \end{array} \right]$$

Zeeman Splitting of Carbon and Aluminum Lines (Single Array)

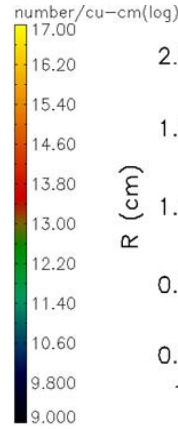
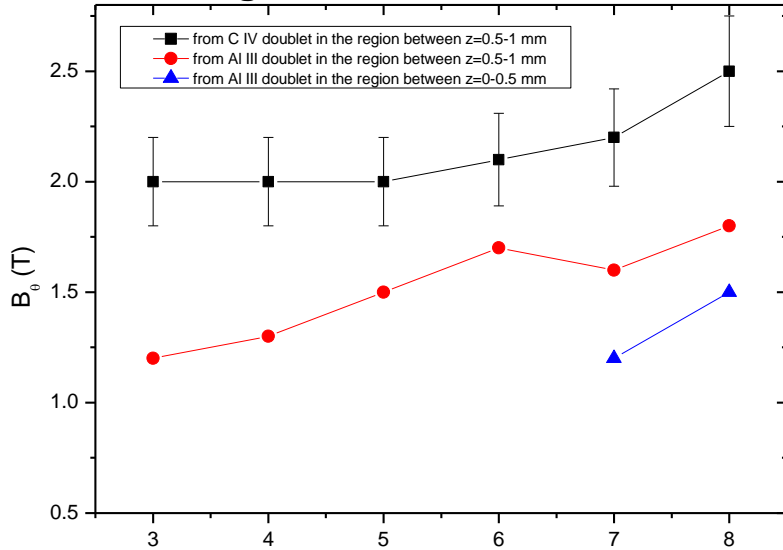


Aluminum and Carbon Line Analysis using Double Fiber Array*

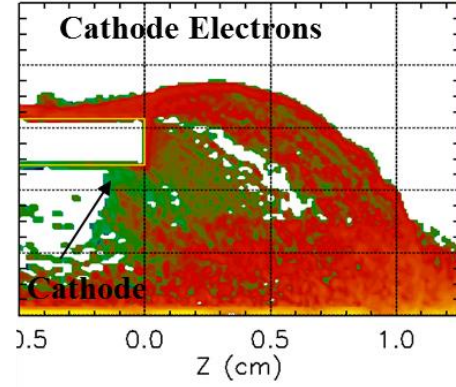
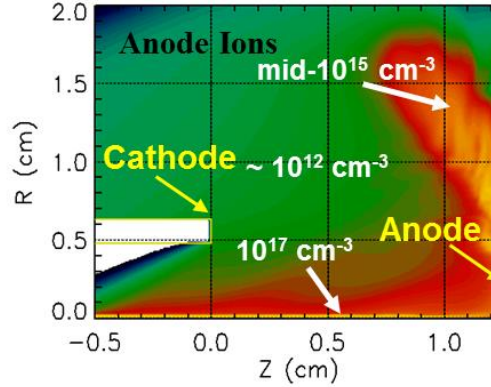


Zeeman Splitting Data Analyses and Conclusions

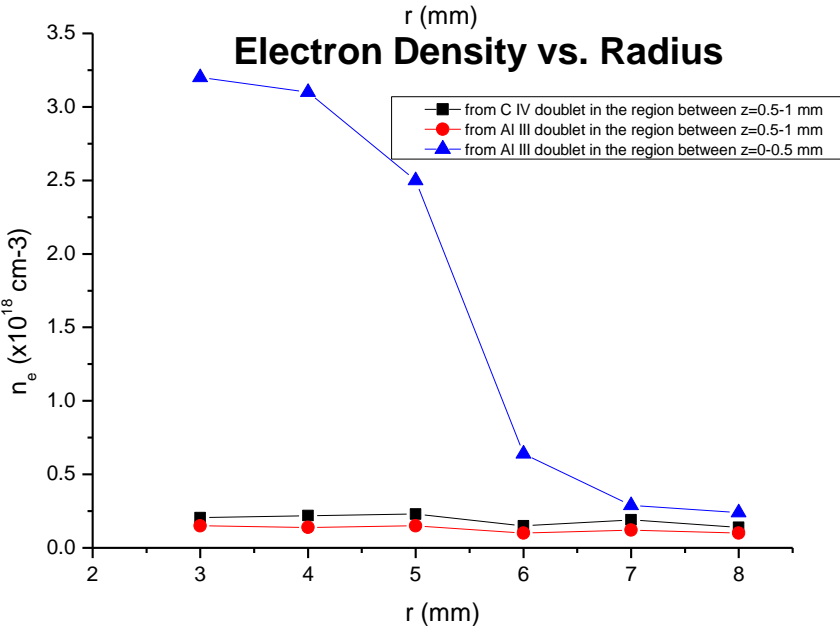
Magnetic Field vs. Radius



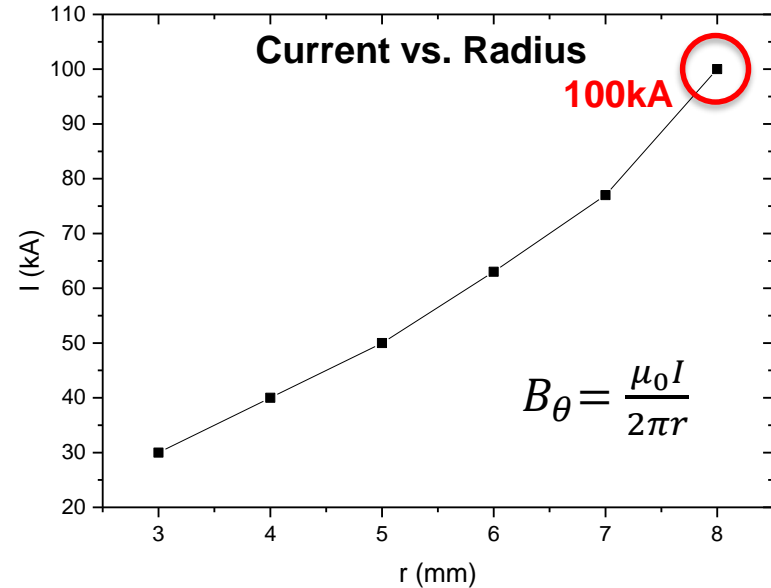
A Ions 40 ns



Electron Density vs. Radius

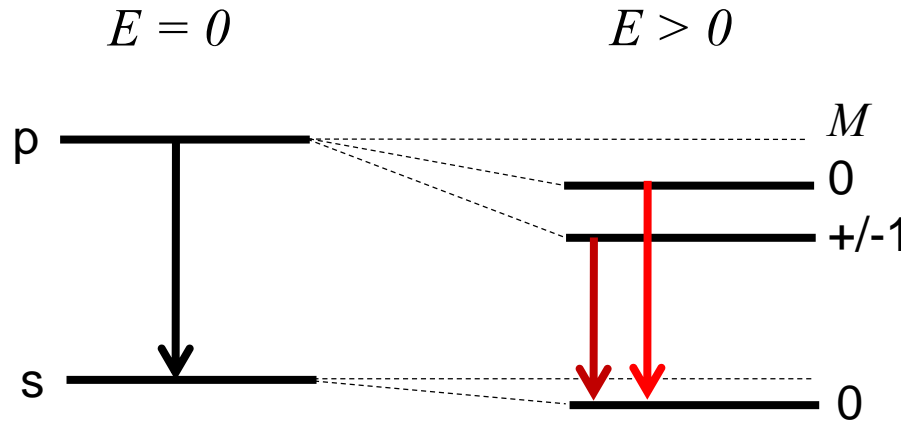
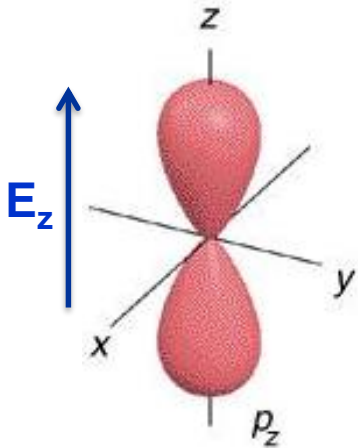


Current vs. Radius



Measurements indicate an enclosed current of 100kA within an 8mm radius. B -dot measurements near the diode region give a total current of 120kA. The additional 20kA may reside outside of the 8mm radius or could be shielded by dense plasma near the electrode surface.

Quadratic Stark Shift is a Useful Technique for Electric Field Measurements in Plasmas

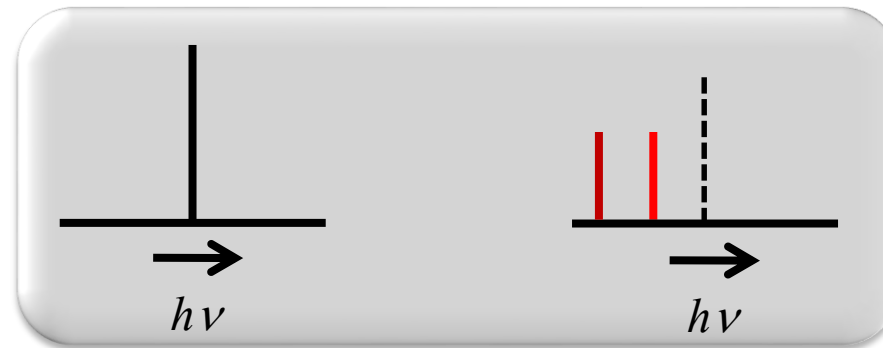


$$\Delta W = -\frac{1}{2} \alpha |E|^2$$

$$\alpha \propto M^2$$

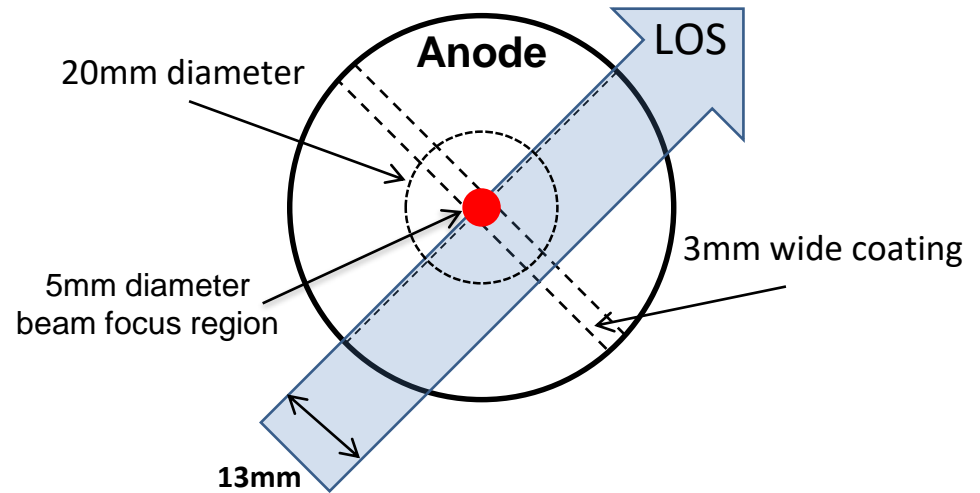
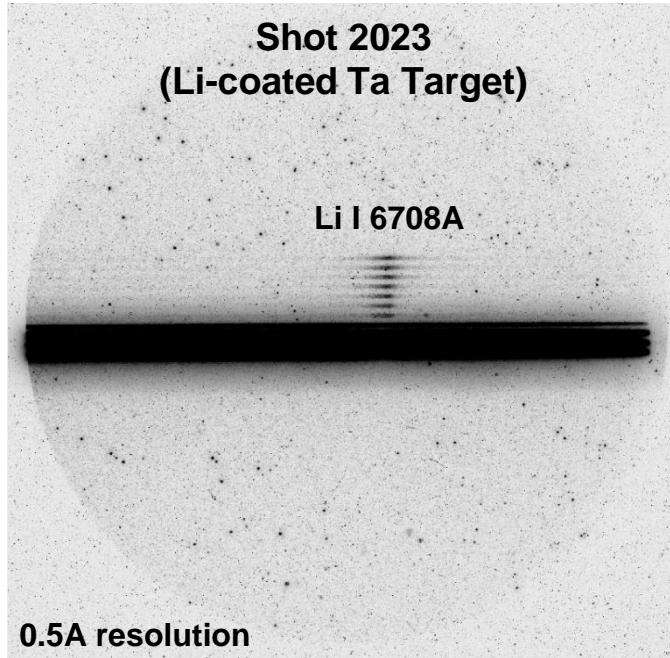
Separation of energy states due to an external E-field inducing a dipole moment in an atom or ion.

Observed

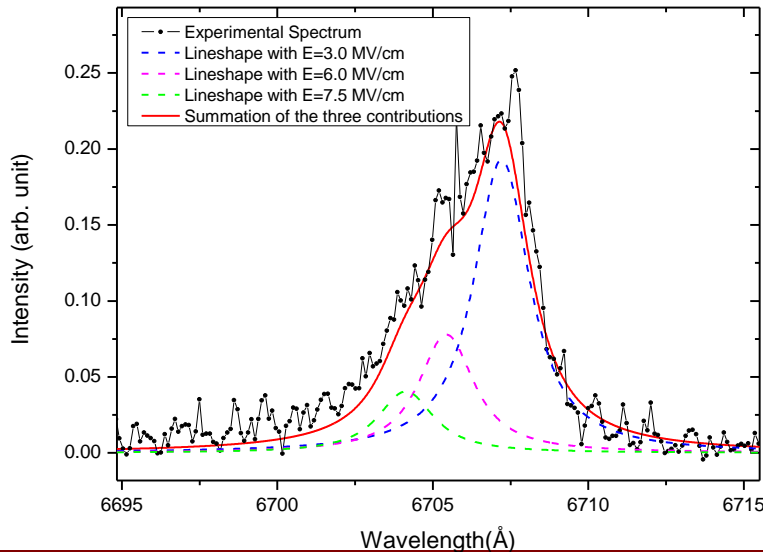


$$h\Delta\nu = h\nu_0 - (\Delta W_u - \Delta W_l)$$

Electric Field Measurements on SMP Diode

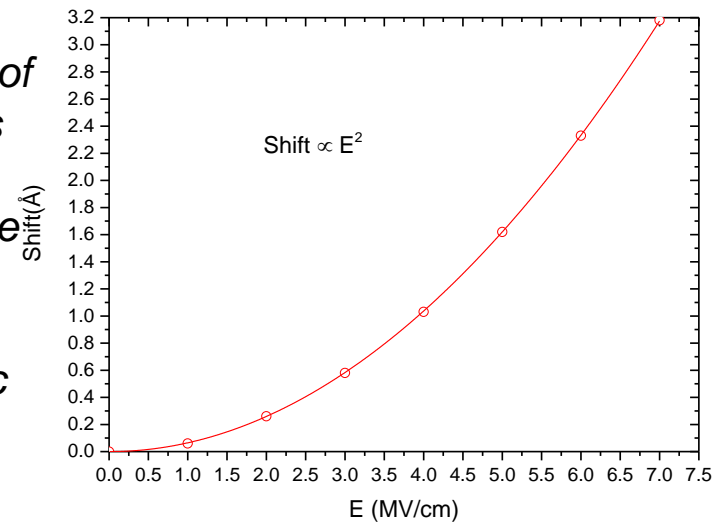


E-fields up to 7.5MV/cm measured on RITS



Large electric fields (MV/cm) cause a shift of the line-center towards shorter wavelengths. Since these spectra are integrated across multiple field lines, the result is an asymmetric line profile skewed towards the blue [4].

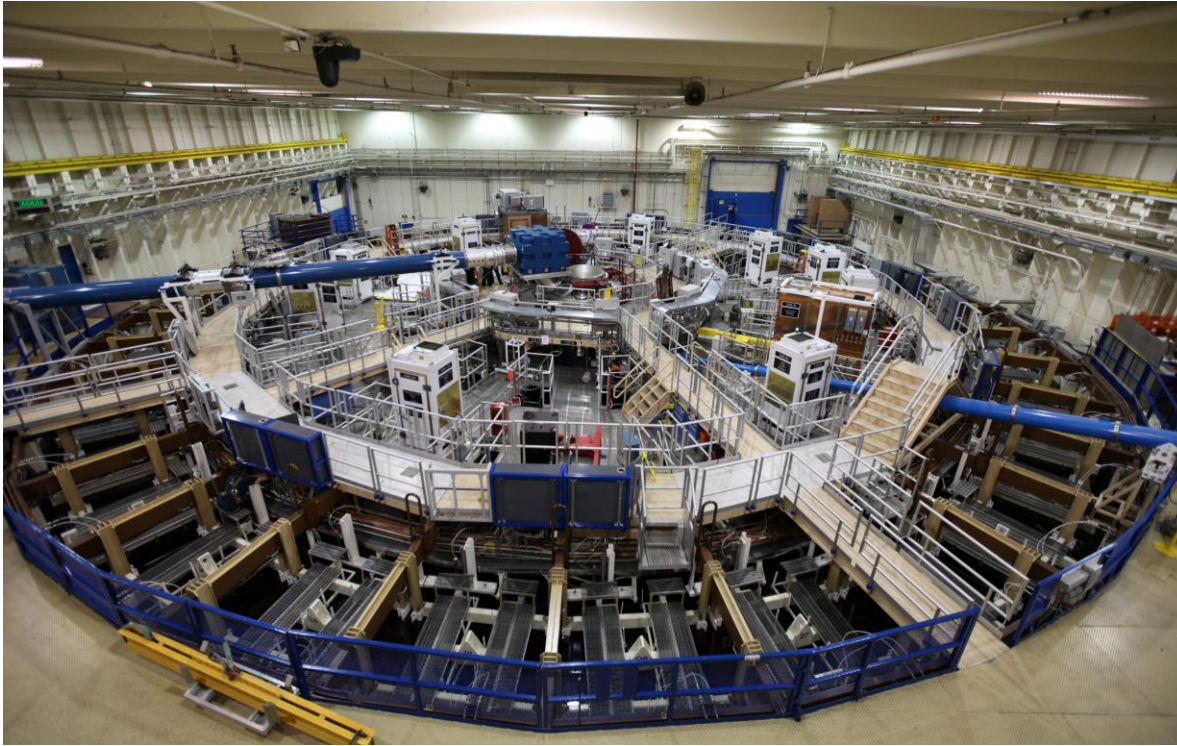
Li I 2s-2p Stark Shifts



Summary of RITS SMP Data

- Measurements of local magnetic and electric fields in the SMP diode have been performed. Changes in the magnetic fields have been determined over very small (0.5mm) spatial extents.
- Measurements of the magnetic field provide information regarding local current distributions in the diode and give indication of return current flow through the plasma.
- A new technique [5], developed at the Weizmann Institute, to measure Zeeman splitting of spectral lines has been employed at SNL on the SMP diode.
- Measurements like these are needed to increase the fundamental physical understanding of plasmas and fields in high power diodes. Until now only global B-fields have been inferred from current probe measurements.
- Present and future understanding and design of high power diodes relies heavily on kinetic PIC and hybrid (PIC/fluid) simulation models.

The Z Machine is the World's Largest Pulsed-Power Driver

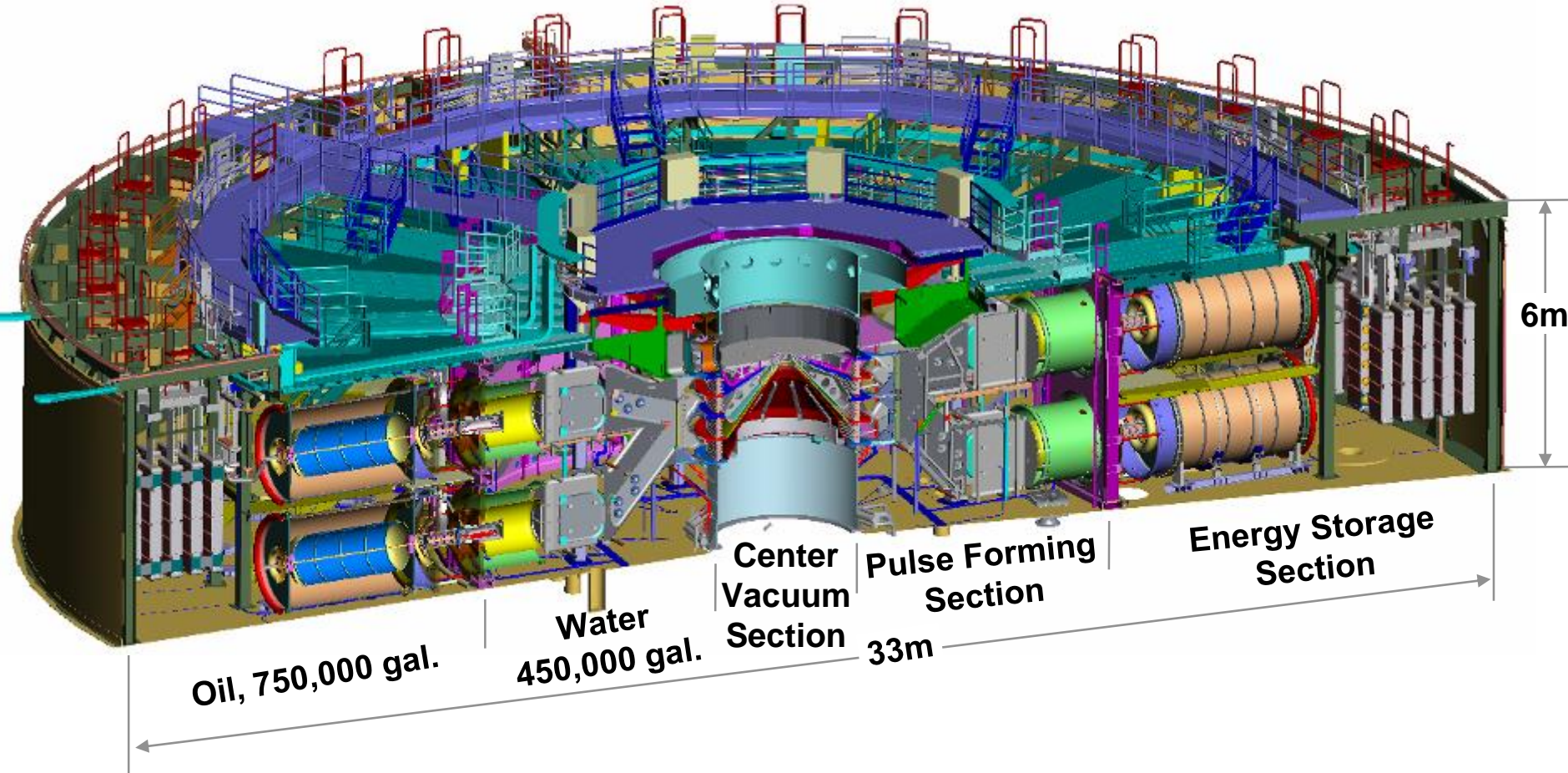


- 22 MJ stored energy
- 3MJ delivered to the load
- 26 MA peak current
- 1-100 Megabar
- 100-600 ns pulse length

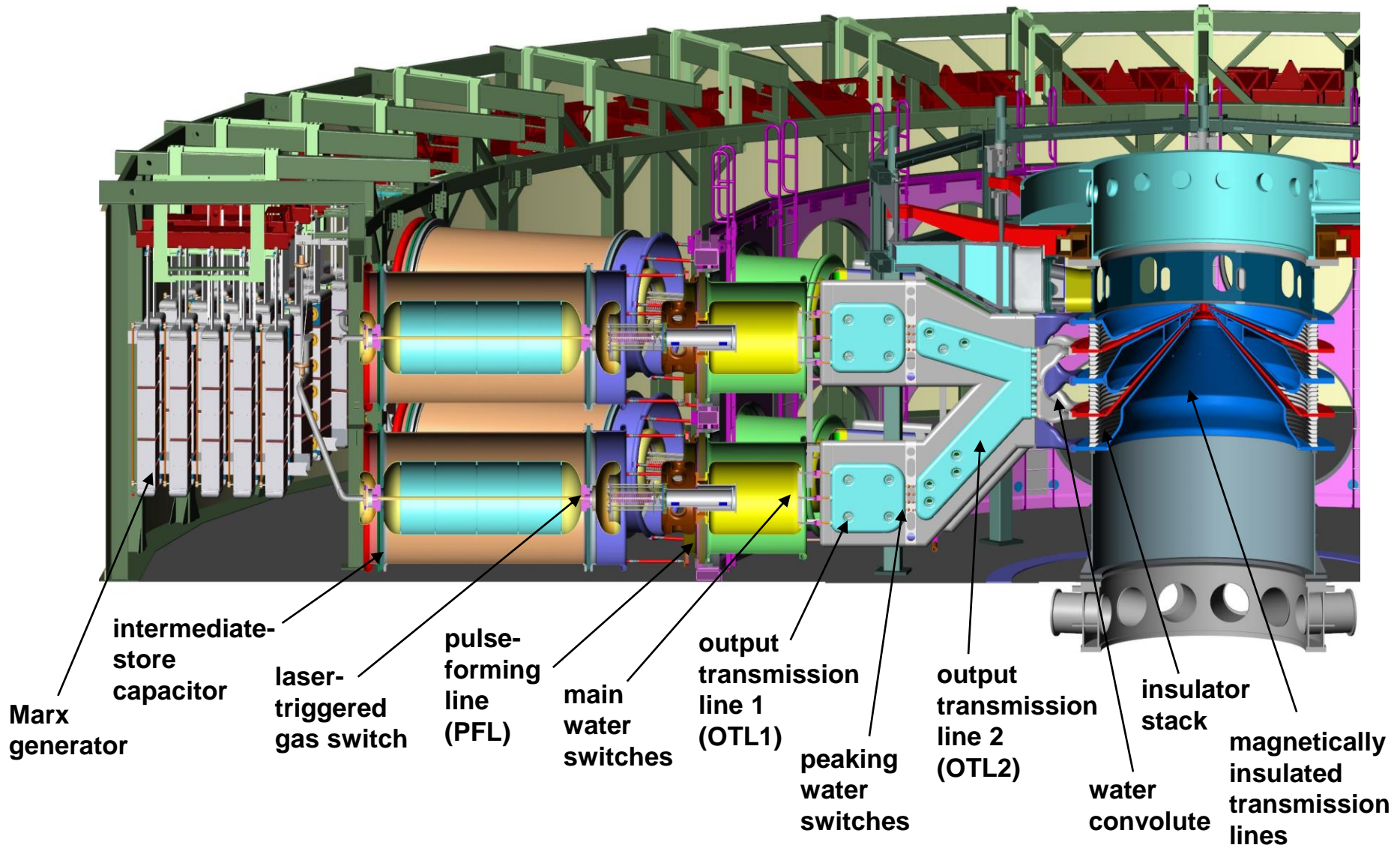
Z Facility

Z is used extensively for NNSA's stockpile stewardship program to study dynamic material properties, radiation effects, and fusion.

Cross sectional view of the Z-machine: 36 individual modules with respective oil, water, and vacuum sections



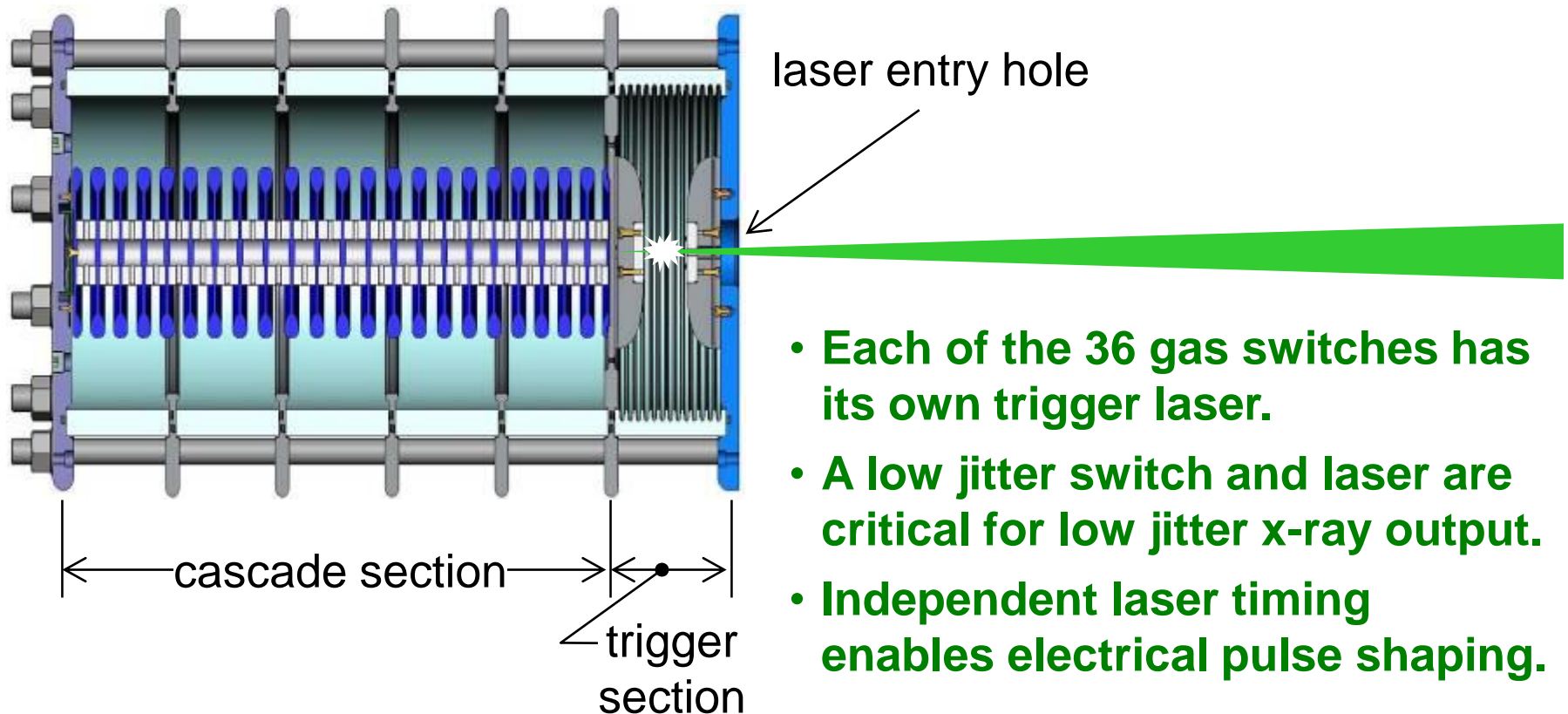
The Z-machine delivers a peak current of 26 MA in ~ 100 nsec



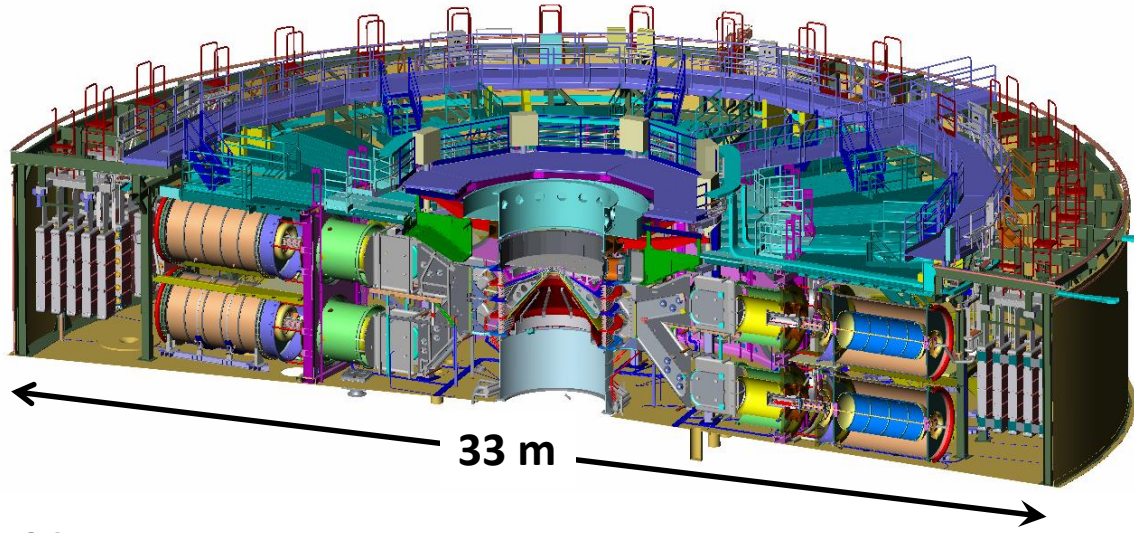
Z Machine: Laser Triggered Gas Switch

Switch filled with ~45 psia SF₆ gas.

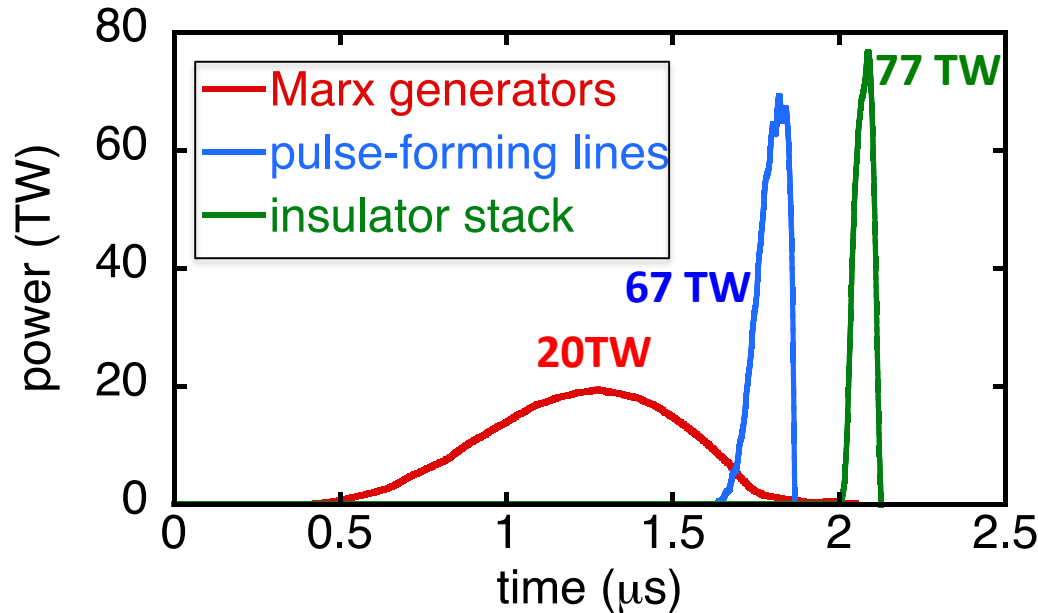
- Each gas switch holds off 6-7 MV and handles 0.75 MA when switched.



Very high pressures can be obtained using the large currents on Z



Z couples several MJ out of 22 MJ stored to the load hardware at the machine center



Magnetically Driven Implosion

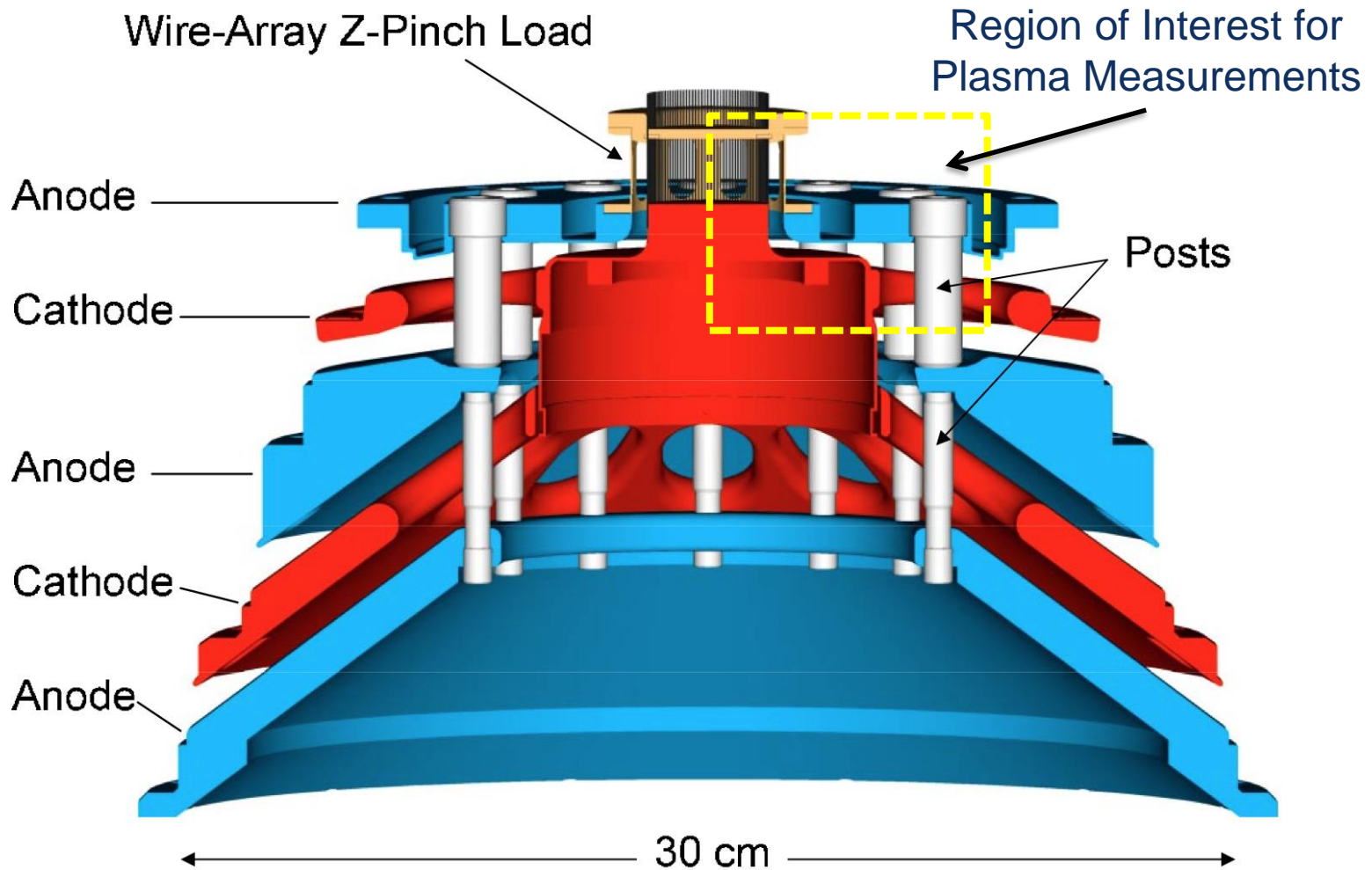
$$P = \frac{B^2}{8\pi} = 105 \left(\frac{I_{MA}/26}{R_{mm}} \right)^2 \text{ MBar}$$

drive current I

R

100 MBar at 26 MA and 1 mm

Z Hardware Configuration [6]



- B-dot measurements are made at 6 cm from the axis
- Vacuum gap decreases to 3 mm in the MagLIF hardware
- Plasma velocity $> 10 \text{ cm}/\mu\text{s}$ measured in the convolute

Motivations for Power Flow Studies on the Z Machine

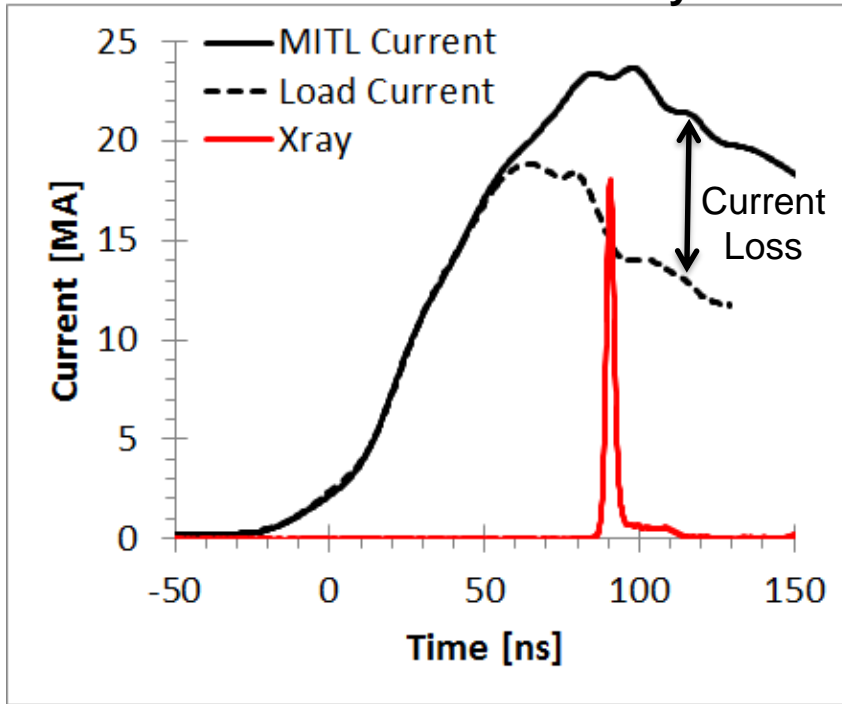
- Obtain measurements of plasmas in the power flow regions on Z for the purpose of gaining a comprehensive physics understanding of plasma formation on Z.
- Detailed plasma measurements have been made on other pulsed-power machines [7]. Want to extend these measurements to the Z-Machine.
- Current losses on Z are attributed to plasmas in the vacuum gap of the final feed section.
- Input experimental data into particle in cell (PIC) codes to better predict plasmas and fields in high power devices.
- Use this information to improve present pulsed power designs, and as a predictive capability for future, next generation facilities such as Z-Next [8].

[7] S.G. Patel, M.D. Johnston, *et al.*, *Review of Sci. Instr.*, **89**, 10D123 (2018).

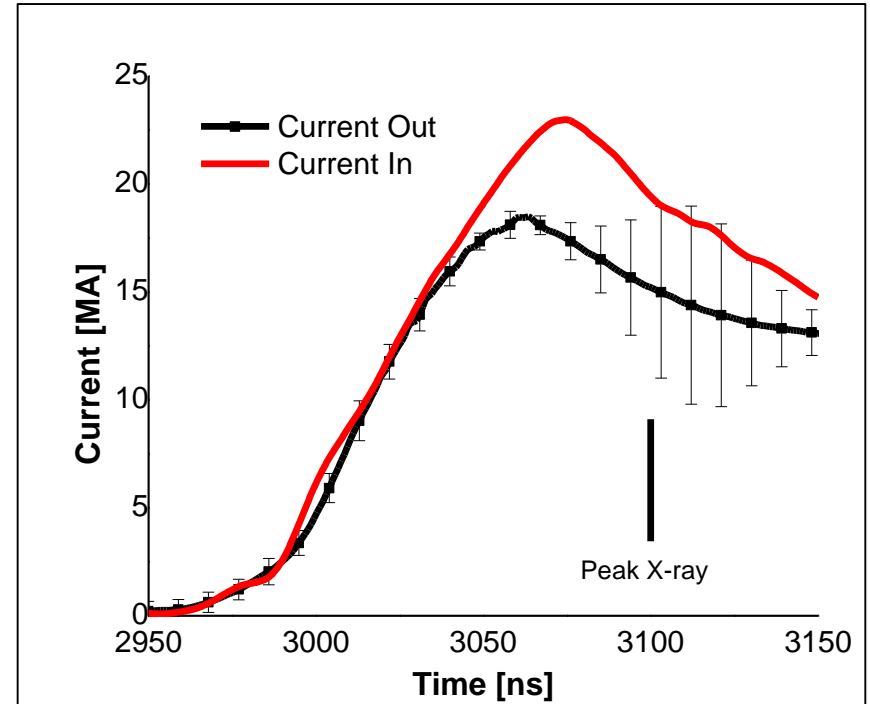
[8] W.A. Stygar *et al.*, *Phys. Rev. STAB*, **18**, 110401 (2015).

Current Losses on Z Reduce Power Delivery to the Loads

Stainless Steel Wire Array

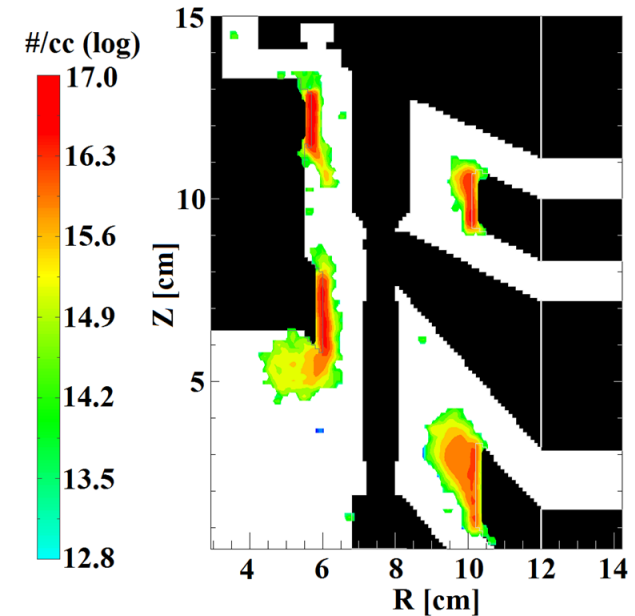
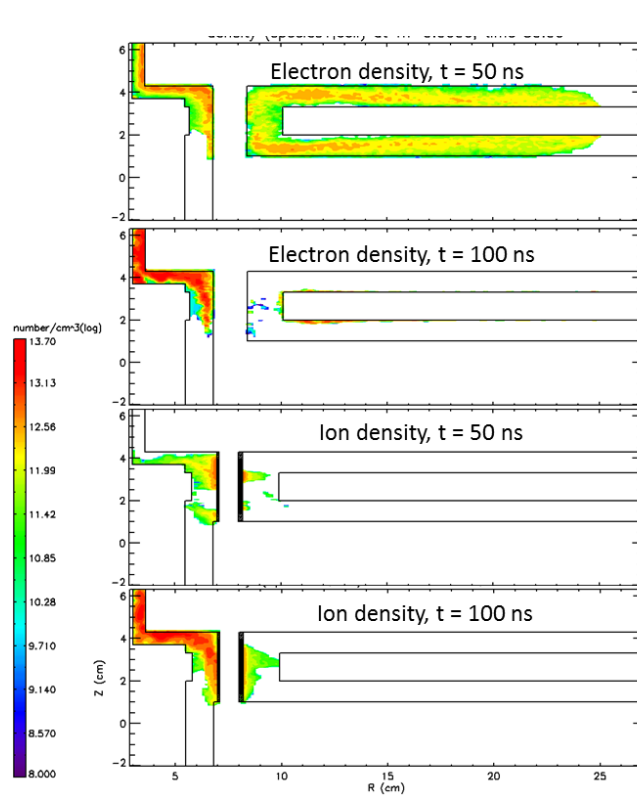


Gas Puff Load

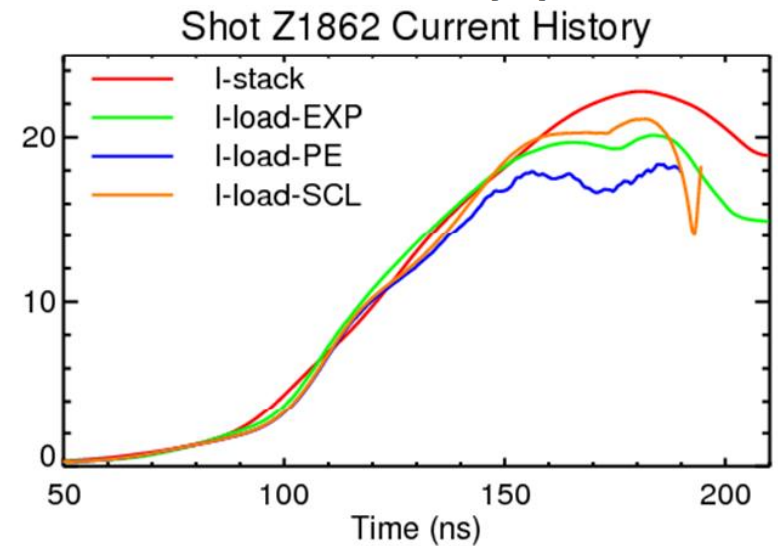


- Up to 5MA current loss is sustained for ~50ns on some loads.
- Surface contaminants, outgassing of electrode materials, and non-ideal geometries affect current delivery to the load.
- Approximately 70% of the total electrical power delivered to the load occurs after peak current, when losses are at their highest.
- Current and voltage near stagnation are more important than the peak current and these are dictated by convolute loss.

Current losses on the Z machine are attributed to plasma formation in the convolute and final current feed [9]



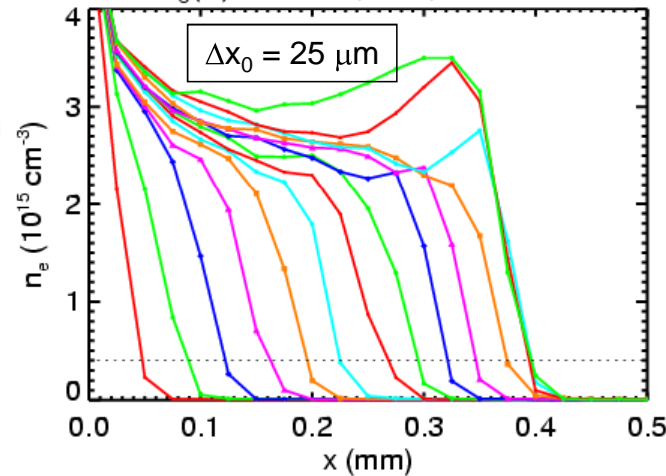
- Plasma models reproduce measured currents, but experimental measurements are needed to verify the physics are correct.



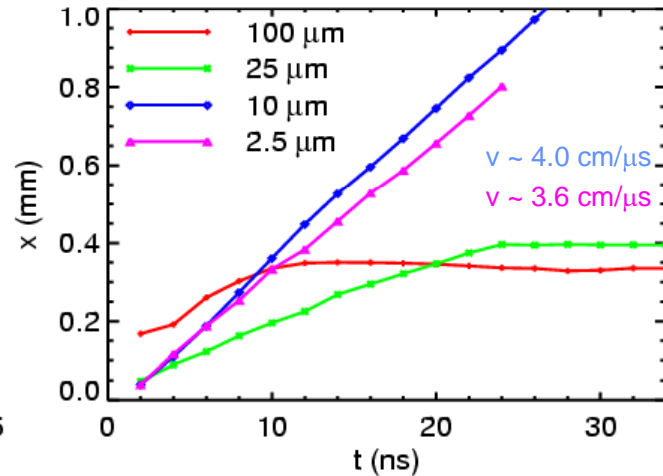
Particle in Cell Modeling of Cathode and Anode Plasma in Quicksilver [10,11]

Cathode Plasma

$n_e(x): t = 2.0, 4.0, \dots, 28 \text{ ns}$

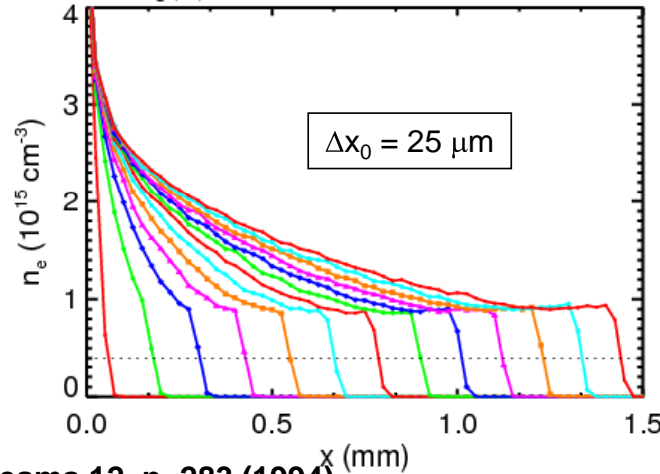


Plasma Front Position

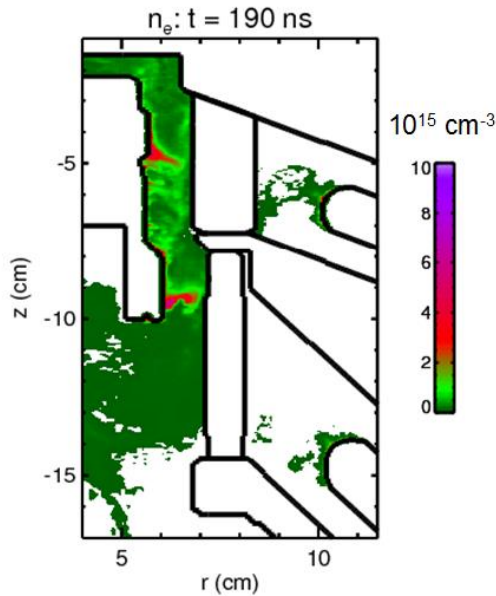
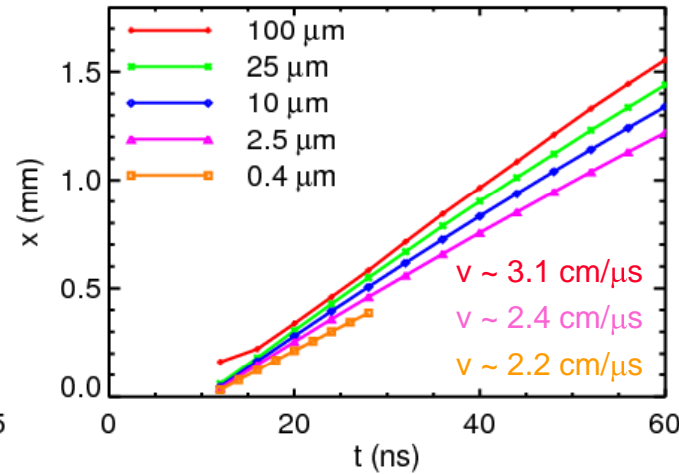


Anode Plasma

$n_e(x): t = 12.0, 16.0, \dots, 60 \text{ ns}$



Plasma Front Position

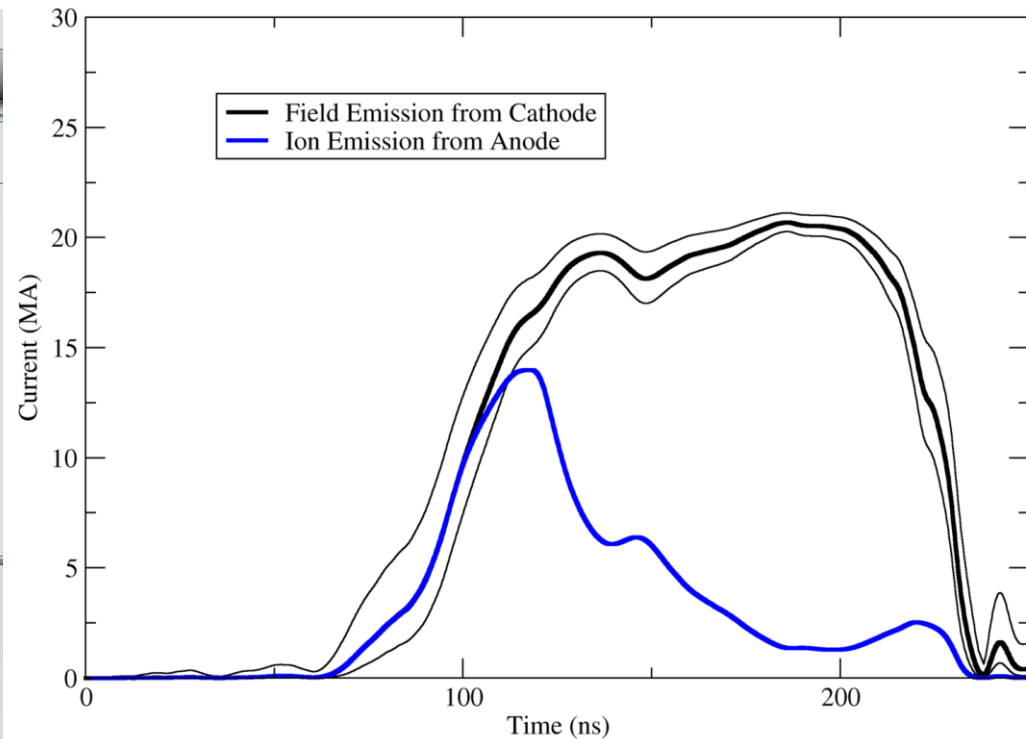
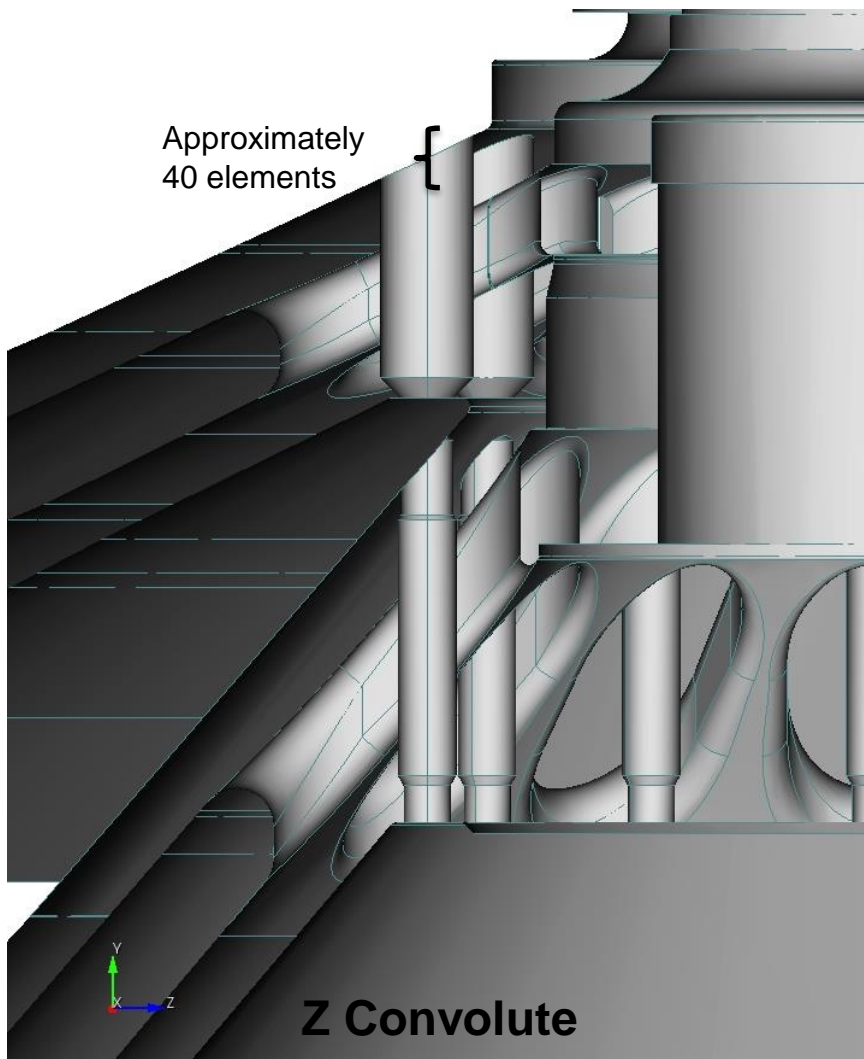


- High density electron structures are observed on the inside of the posts, where B-fields are high.

[10] J.P. Quintenz, *et al.*, *Laser Part. Beams* **12**, p. 283 (1994).

[11] T.D. Pointon, *52nd Annual Meeting of the APS Division of Plasma Physics*, Nov. 8-12, 2010.

EMPHASIS simulations are focused on final-feed gap and provide guidance for plasma experiments [12]

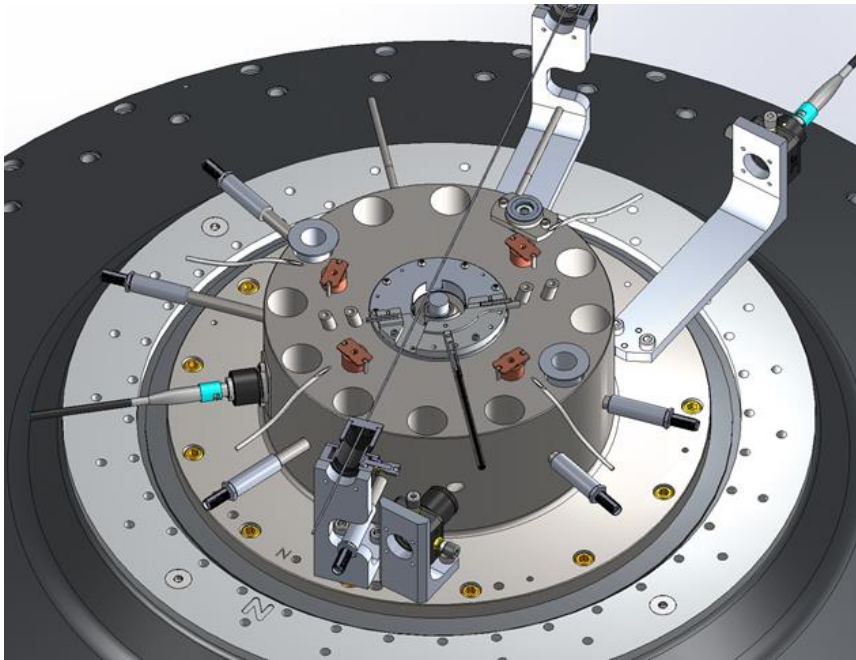


Initial bounding calculations of geometry

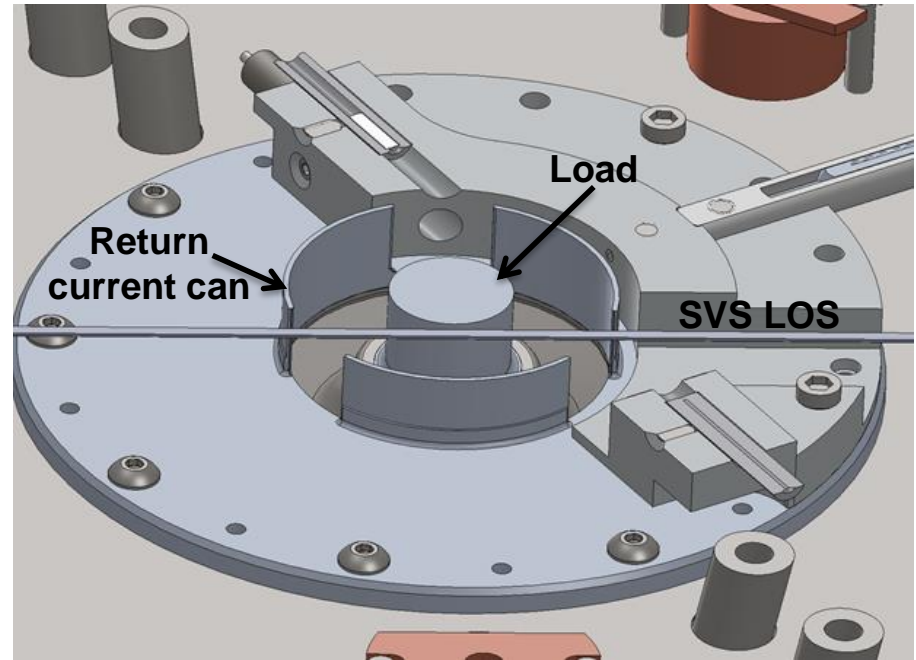
- Showing best, **largest** current case with uncertainty (black)
- Showing **lowest** current case (blue)

[12] Slide courtesy of Keith Cartwright (SAND Report: SAND2017-12565, Johnston, et. al.).

Dedicated Experiments for Power Flow Physics are now Being Conducted on Z

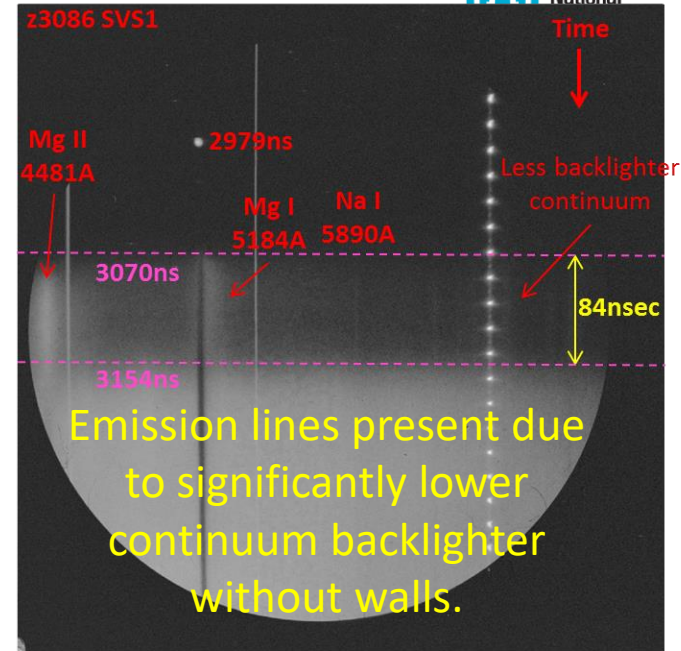
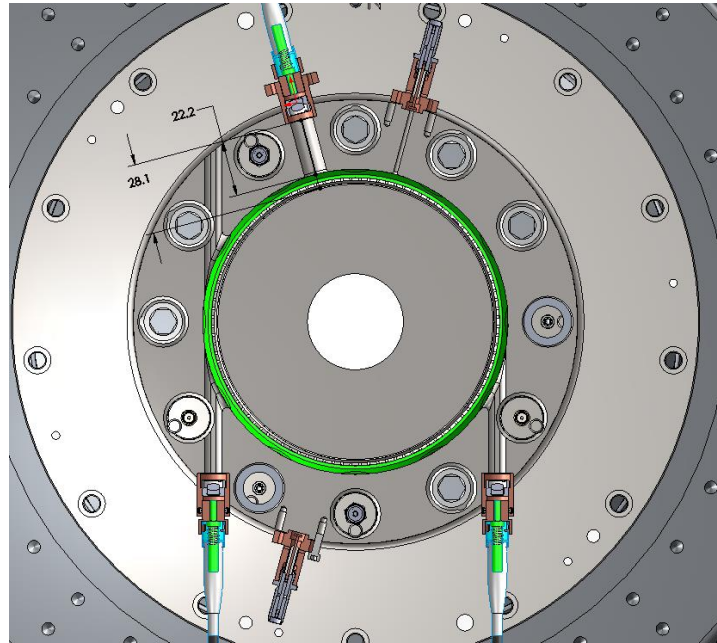
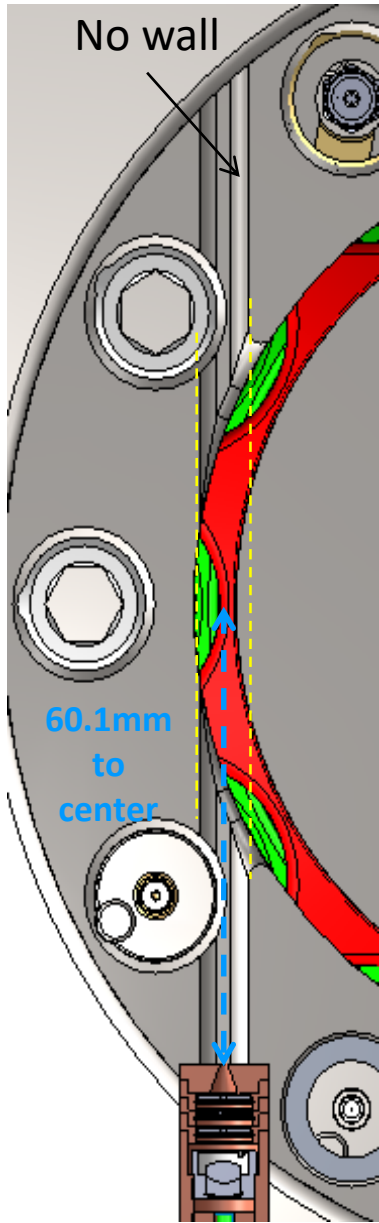


Power Flow Hardware

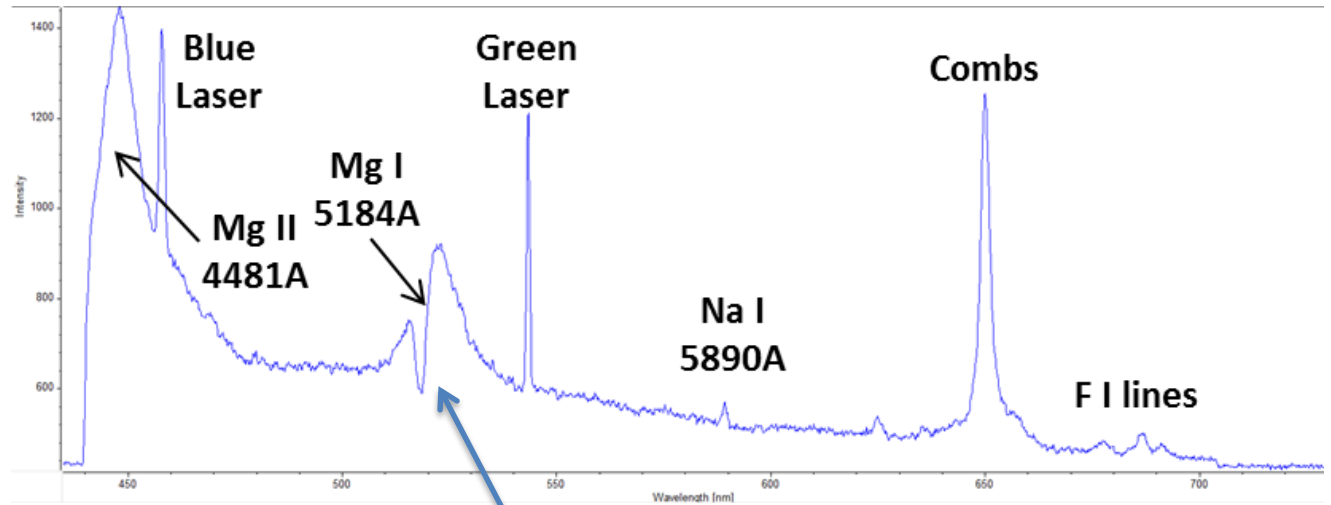


- Experiments are designed to look for plasmas off the surface of a non-impinging load.
- Coatings are applied to the load to measure specific neutral and ion lines.
- Experiments are designed to look in the final feed gap without a backlighting wall.

Chordal Line of Sight on Power Flow Shots in the Final Feed



*20nsec combs

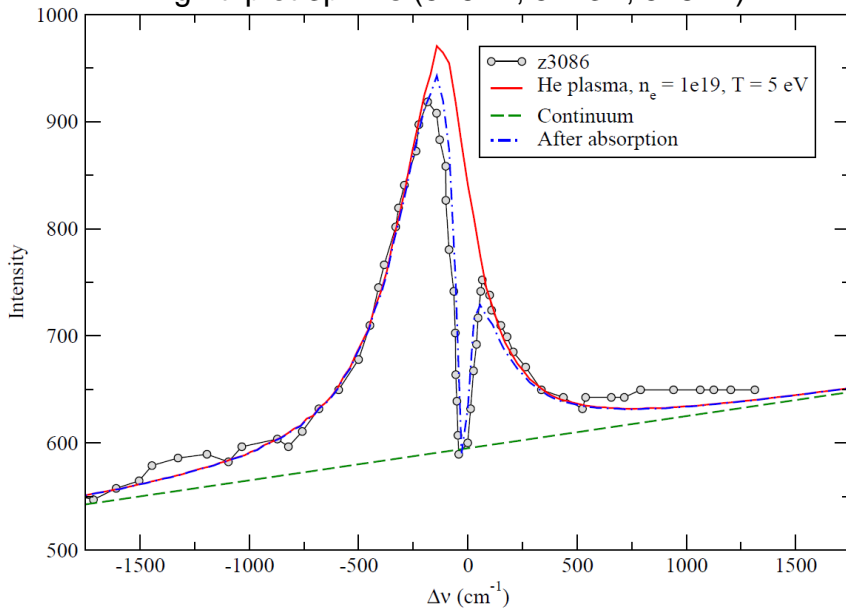


Emission and self-absorption of Magnesium neutral observed.

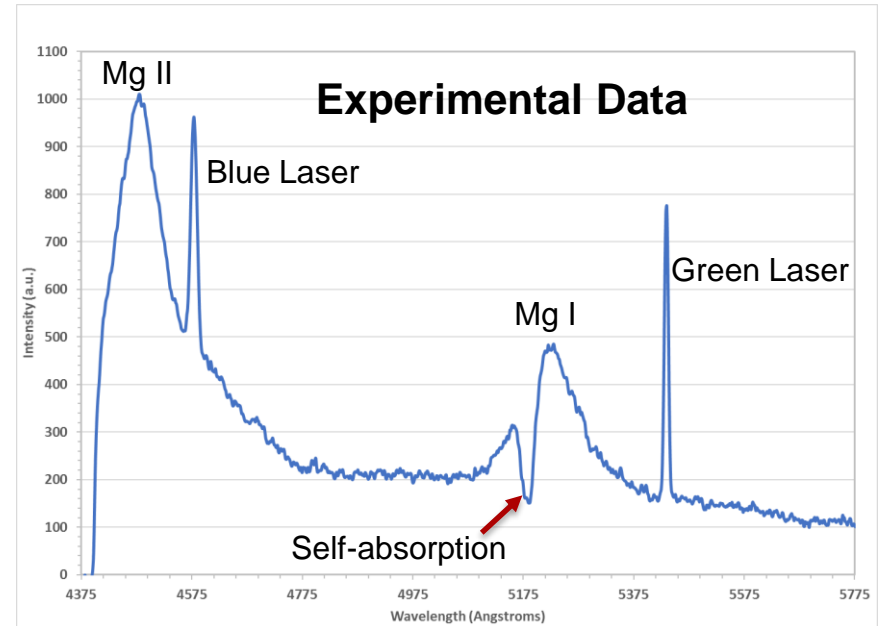
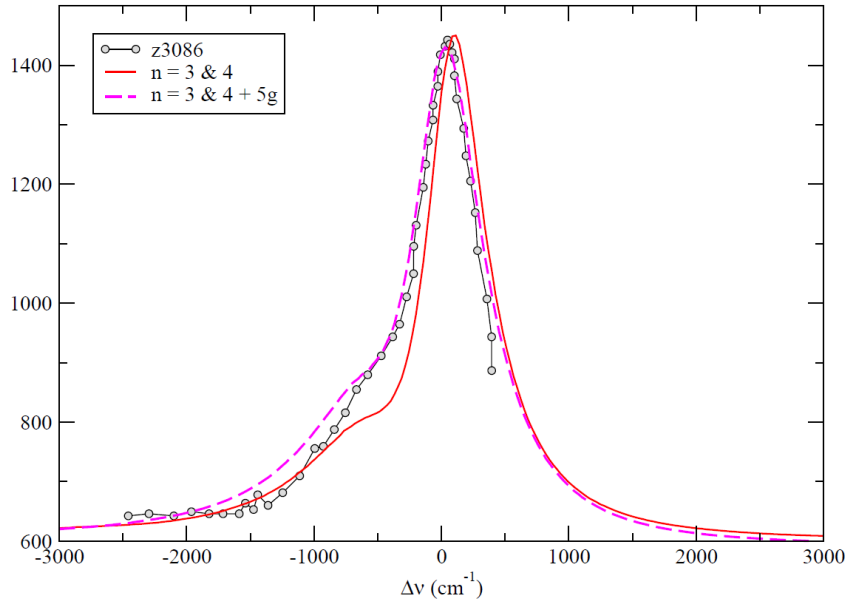
Magnesium Dopant Results

- MgF_2 coated optics
- Mg I and Mg II broadened line emission observed
- Two distinct plasma regions present in spectrum
- Colder, more dilute Mg I plasma next to optics
- Hotter, denser plasma, further off the surface
- Light from the hotter, denser plasma is absorbed in the cooler plasma.
- Density of emitting plasma: $\sim 1 \times 10^{19} \text{ cm}^{-3}$
- Density of absorbing plasma: $\sim 1 \times 10^{18} \text{ cm}^{-3}$
- Plasma temperatures: 1-5 eV
- Mg I lines are red-shifted by 5.9 \AA
- Opacity (τ) = ~ 0.4
- $1 \times 10^{19} \text{ cm}^{-3}$ continua fits experimental data

Mg I triplet 3p - 4s (5167Å, 5173Å, 5184Å)



Mg II 3d - 4f (4481 Å)
He plasma 5 eV, 10^{19} cm^{-3}



Metastable level in Mg I (steady state, without opacity)

$3s3p\ ^3P$ - metastable level

$3s3p\ ^3P \rightarrow 2p6\ 3s2\ ^1S$ - spin-forbidden transition

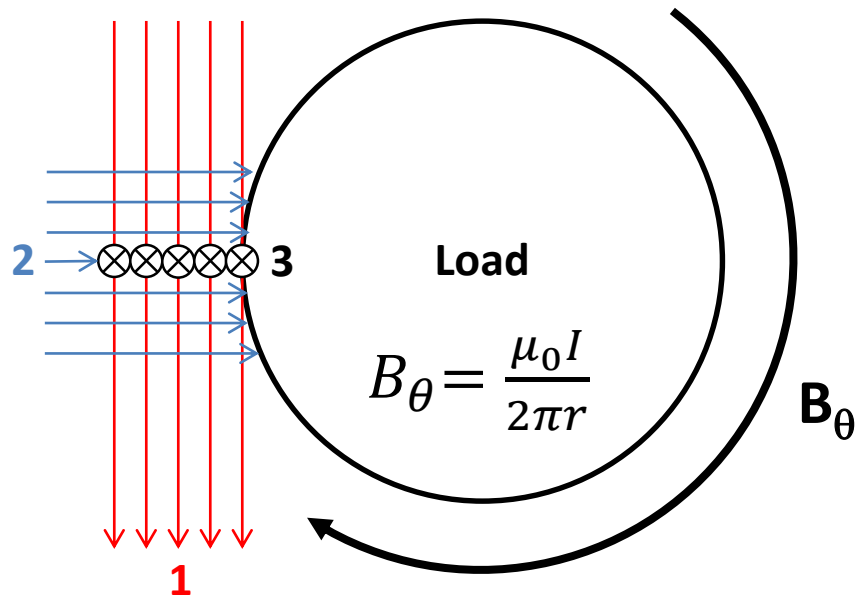
$3s4s\ ^1S \rightarrow 3s3p\ ^1P$; $\lambda = 11,828\ \text{\AA}$ (NIST)

$3s4s\ ^3S \rightarrow 3s3p\ ^3P$; $\lambda = 5,183\ \text{\AA}$ (NIST)

| T_e (eV) | Level | N_e (cm ⁻³) | POP* | $A_{i \rightarrow j}$ *** |
|------------|---------------------------------------|---------------------------|----------------------|---------------------------|
| 1 | $3s4s\ ^1S$ | 10^{19} | $1.62 \cdot 10^{-3}$ | |
| | $3s4s\ ^1S \rightarrow 3s3p\ ^1P$ | | | $2.85 \cdot 10^{+7}$ |
| | $3s3p\ ^1P \rightarrow 2p6\ 3s2\ ^1S$ | | $1.39 \cdot 10^{-2}$ | $5.05 \cdot 10^{+8}$ |
| 1 | $3s4s\ ^3S$ | 10^{19} | $6.47 \cdot 10^{-3}$ | |
| | $3s4s\ ^3S \rightarrow 3s3p\ ^3P$ | | | $1.23 \cdot 10^{+8}$ |
| | $3s3p\ ^3P \rightarrow 2p6\ 3s2\ ^1S$ | | $2.13 \cdot 10^{-1}$ | $5.01 \cdot 10^{+1}$ |
| 1 | $gs^{**} - 2p6\ 3s2\ ^1S$ | 10^{19} | $3.57 \cdot 10^{-1}$ | |

Zeeman Splitting Measurements on Z

Three Potential Views at the Load



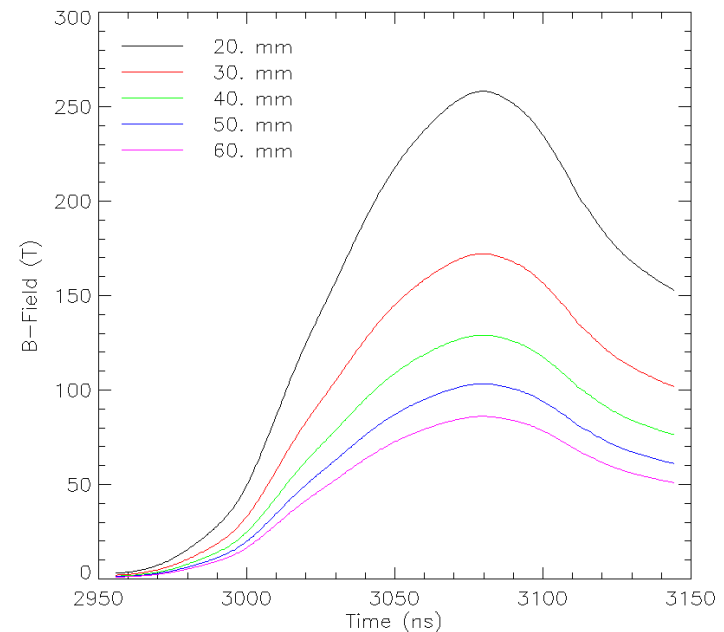
Considerations:

- Polarizations (σ and π)
- Lines of sight vs. B-field orientation
- Weak field/Strong field
- Specific Lines (low Stark)
- Plasma density and temperatures
- Doppler broadening

Requirements:

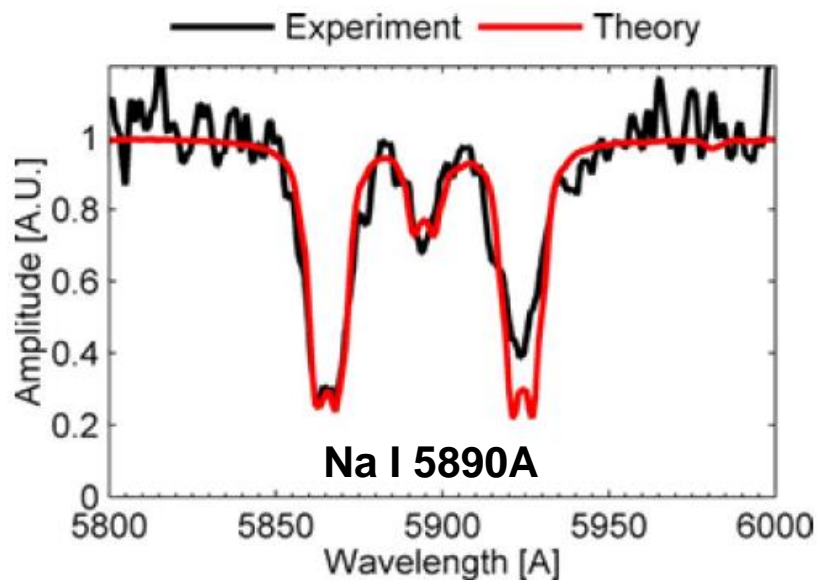
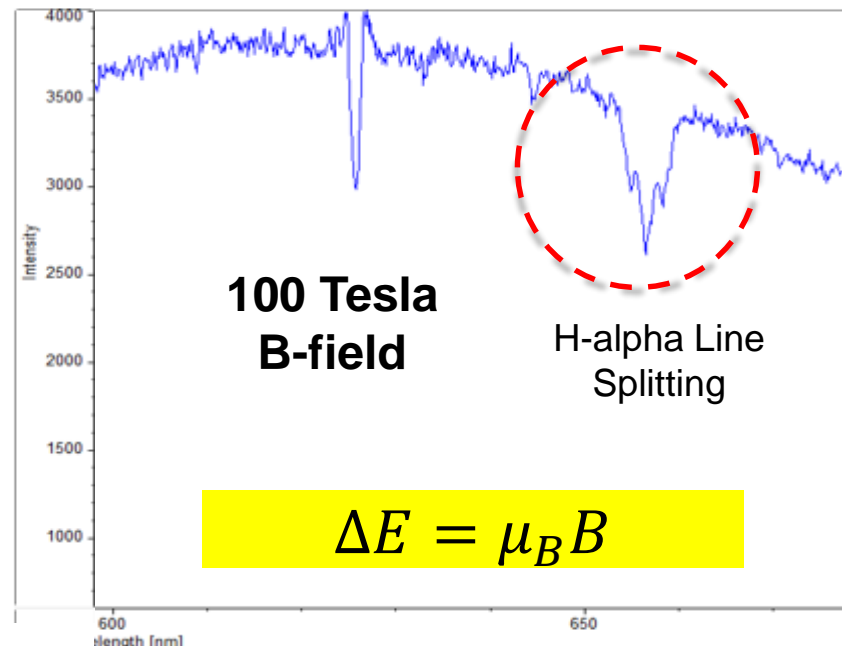
- Slotted return current can
- Multifiber array
- Detectors (Streaked spectra, gated spectra, photodiodes)
- Dopants (Na, Li, Al, C, others)
- Compare with VISAR measurements at the load
- Compare with B-dot monitors at $r=6\text{cm}$

B-field versus Radius



Zeeman Splitting on Z

- Time and space resolved Zeeman measurements were taken on the SMP diode on RITS-6 as a proof of principle for Z.
- Calculations of Zeeman lineshapes have been done for Al III and C IV covering a wide variety Z relevant temperature and density regimes.
- Previous work by Gomez et. al. measured Na I splitting in the load region on Z [13].

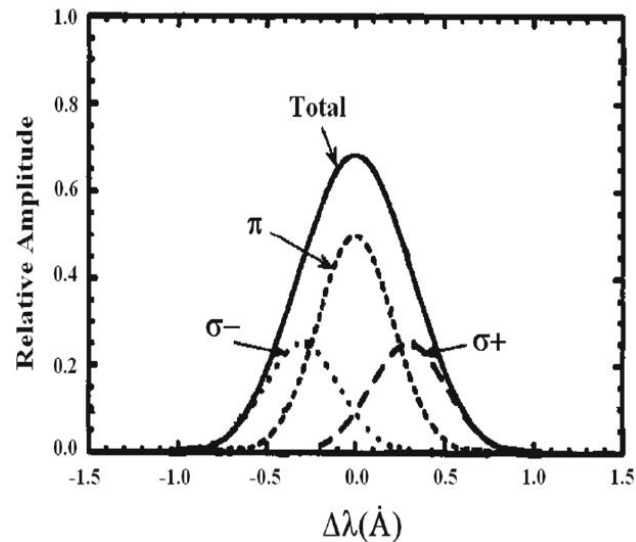


$$\lambda_0 = 6563 \text{ \AA}$$

$$\Delta\lambda = 1.2 \text{ \AA/T}$$

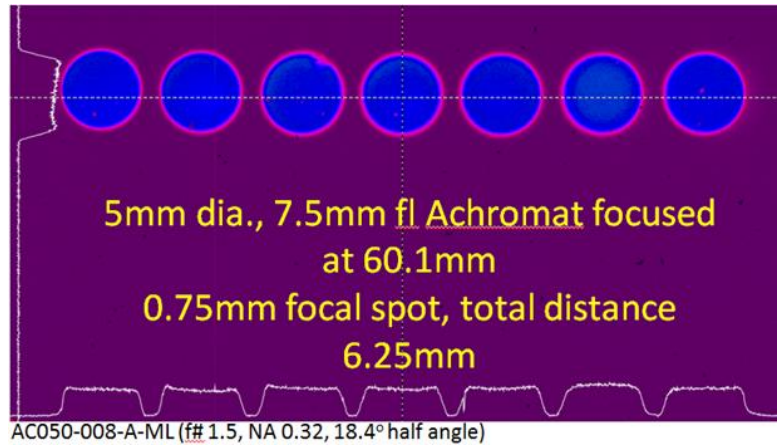
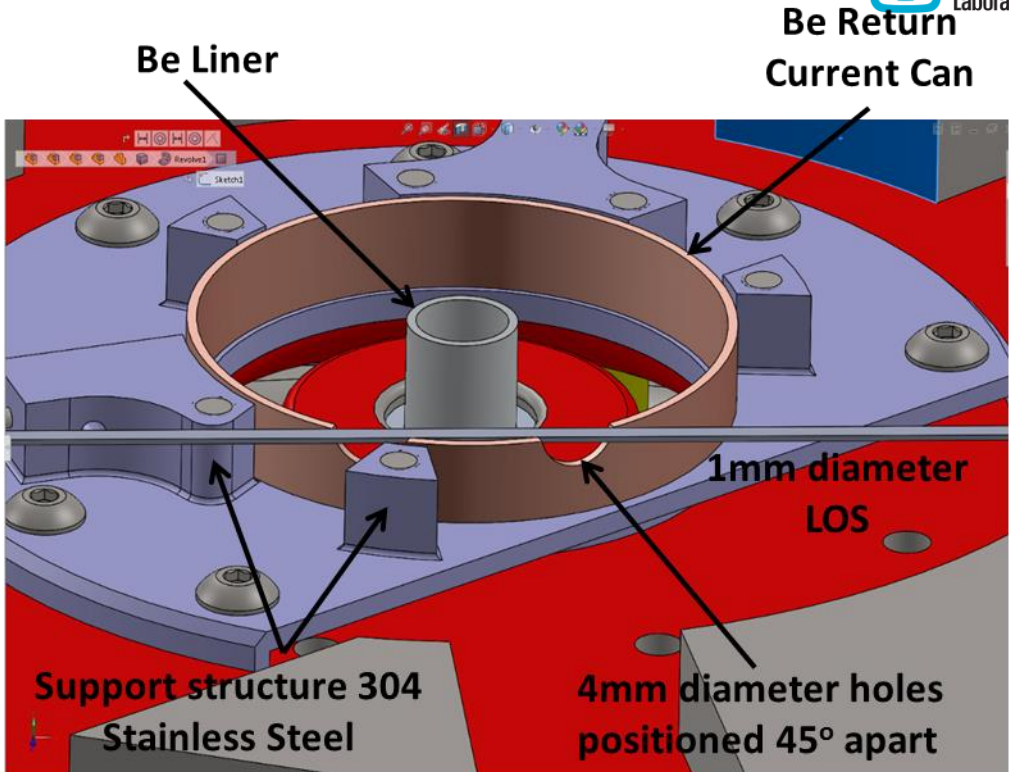
$$m = 0, \pm 1$$

$$B = 100 \text{ T}$$

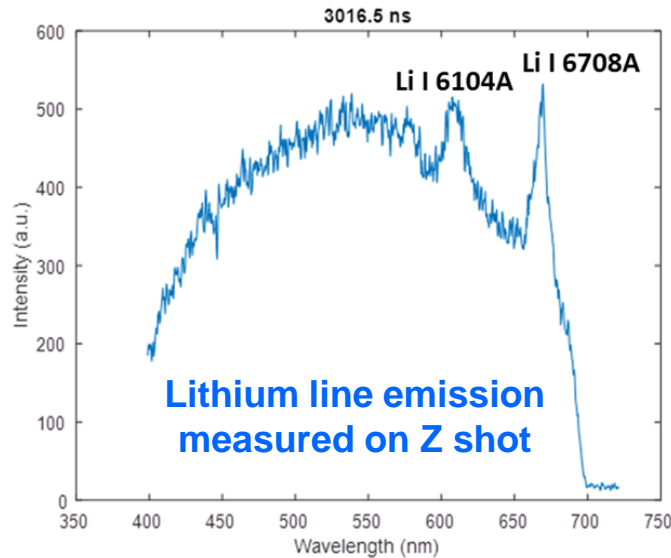


Proposed Zeeman Splitting Measurements Inside the MagLIF Return Current Can

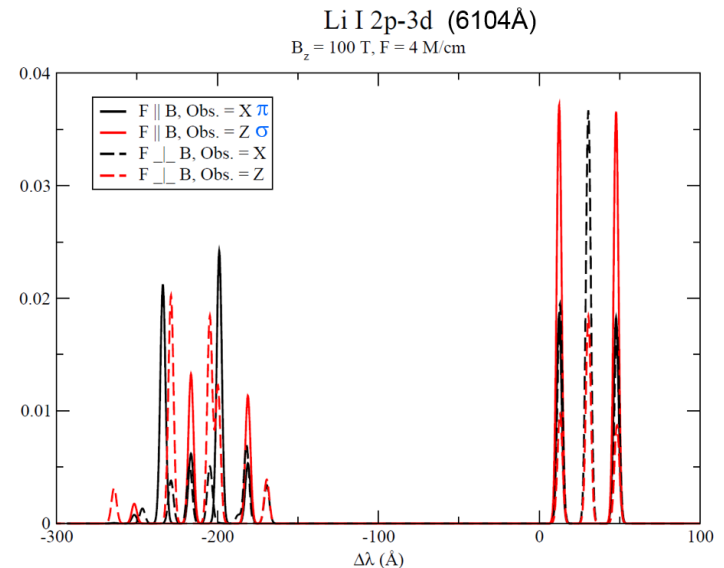
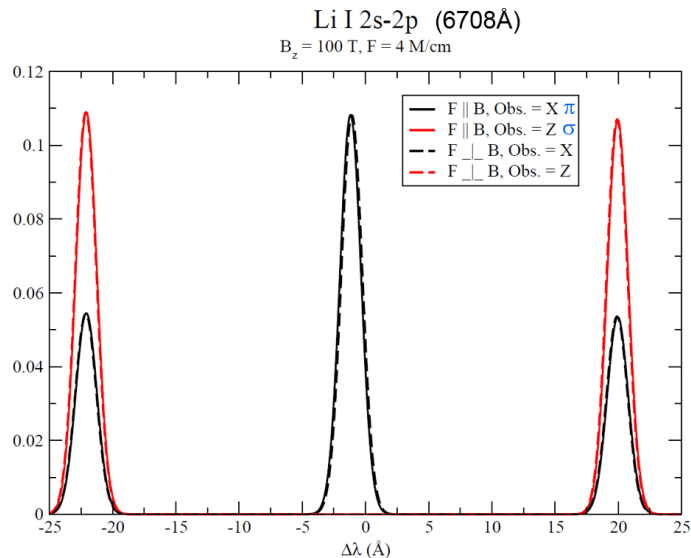
- Dopants will be applied to the inside of the return current can, around the holes.
- A horizontal array of fibers will be used to allow for measurements at different distances.
- Various dopants will cover both neutral and ion species.



Lithium Dopant for Electric and Magnetic Field Measurements

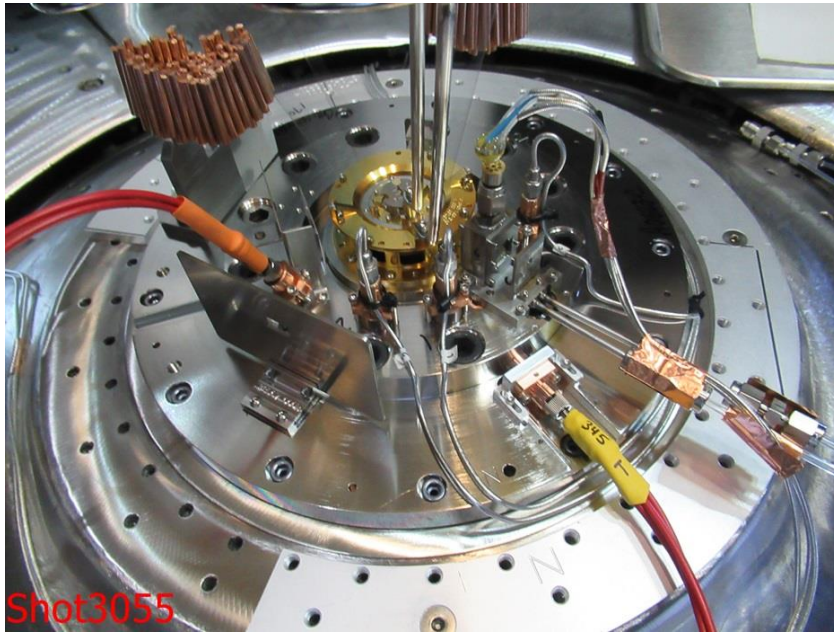


Lithium neutral lines (6708Å and 6104Å) used in combination, provide a means of measuring local electric and magnetic fields in Z power flow regions.

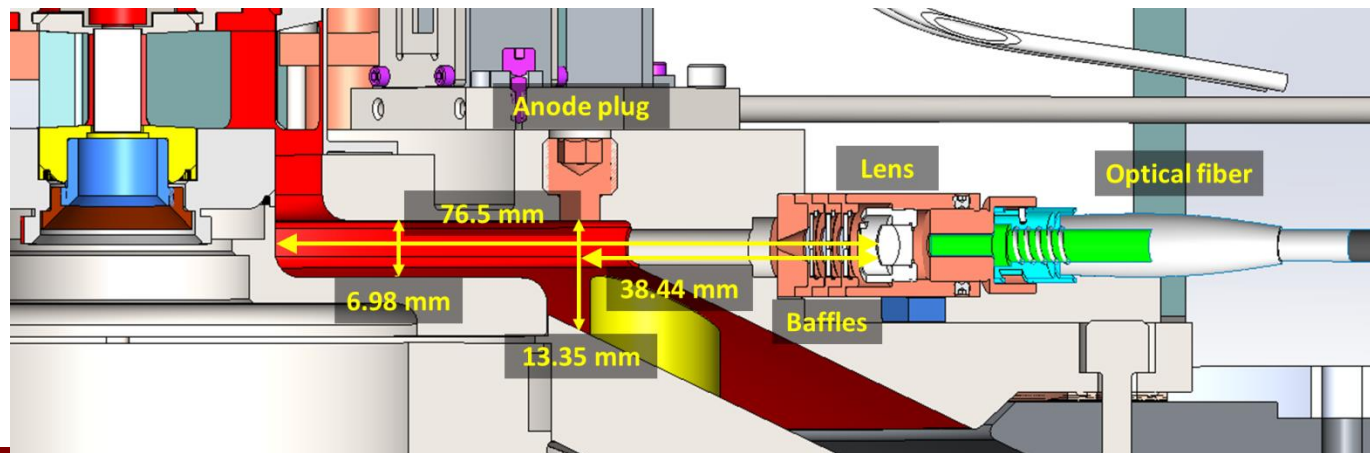
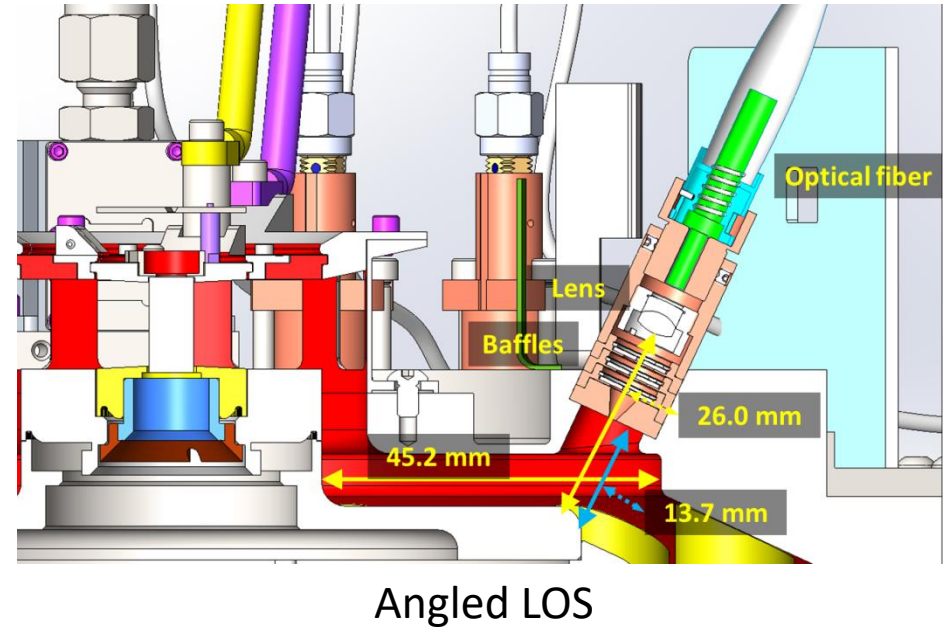


- Current distribution is important in the design of new pulsed-power machines and in the understanding of existing machines (ex. Z).
- The only way to obtain line emission from the A-K gap of a power-flow transmission line is to use neutrals, which requires:
 - Sufficient number of neutrals in the gap
 - Using neutrals that are not field-ionized in the gap, or more precisely, the atomic level of interest (that provides the radiative decay) should not be field ionized.
- In order to observe the Zeeman effect, one needs line emission in the gap that is not Stark shifted.
- To prove the neutral atoms emitting the line(s) are in the gap (rather than in the plasma) one also needs an emission line from the same atom that is Stark shifted.
- We proved, both experimentally and theoretically, that Li neutrals fulfill these requirements, namely:
 - The 2p-2s transition is not Stark shifted and demonstrates the Zeeman effect.
 - The 3d-2p transition is Stark shifted and proves the presence of the emitting neutrals in the gap.
 - The upper, n=3 level of Li I (also the 2p level) does not field ionize in the gap.
- **In Summary, we demonstrated a promising method to reliably determine the current distribution in the final feed section on Z.**

Ride-along Experiments are Fielded on Multiple Z Platforms

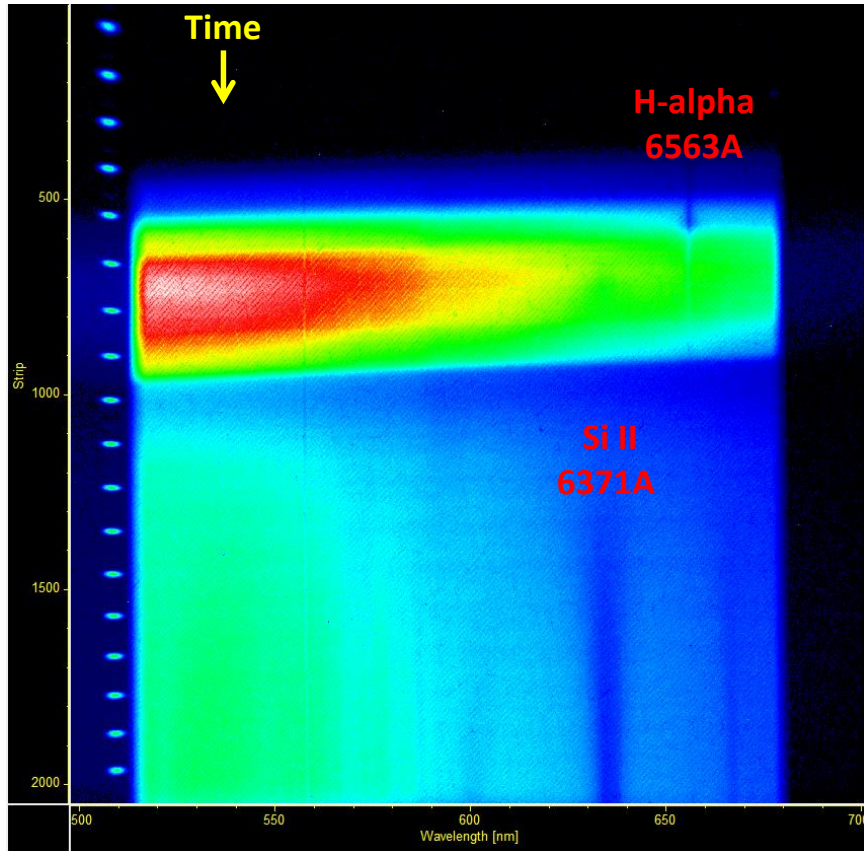


Wire Array Experiment

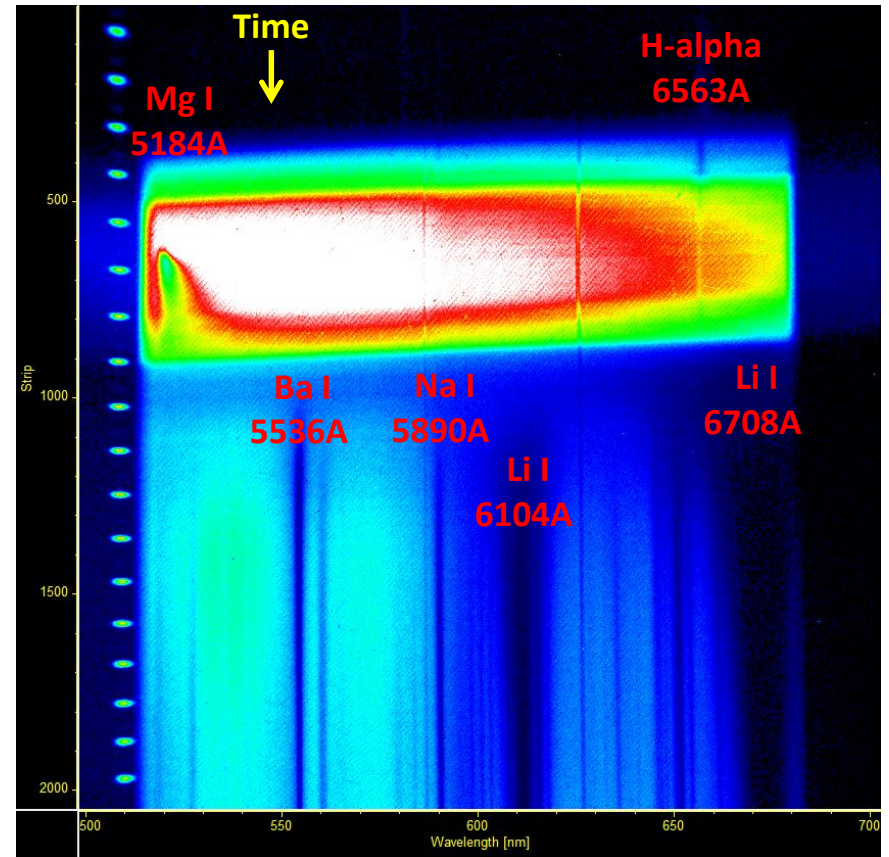


Horizontal LOS

Spectra from Nested Wire Array Experiments



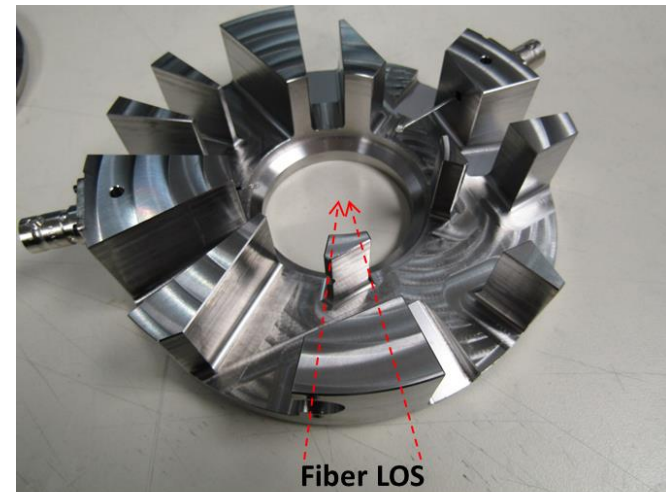
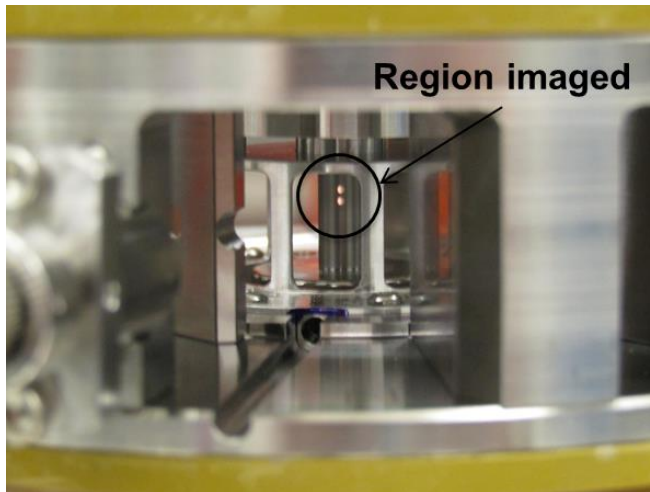
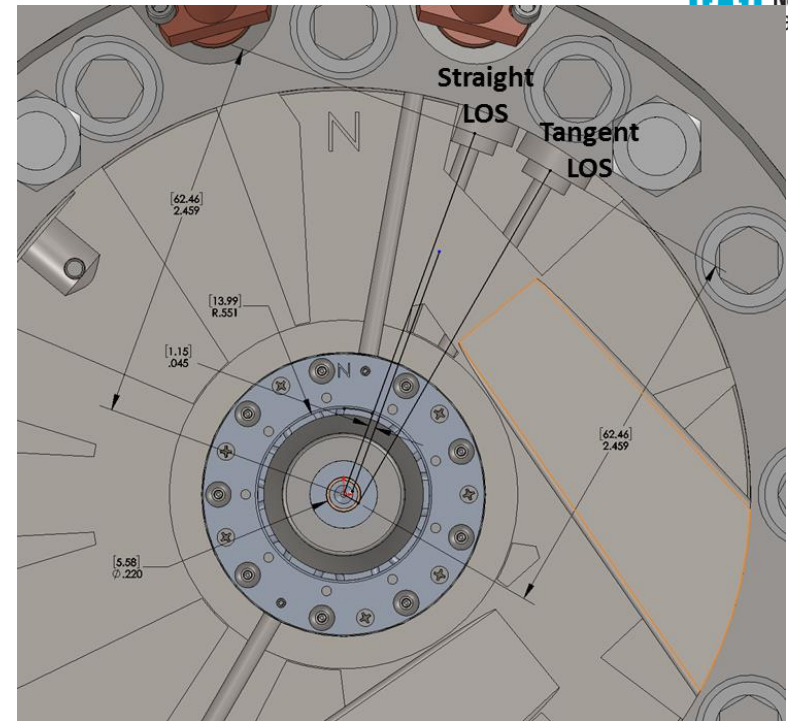
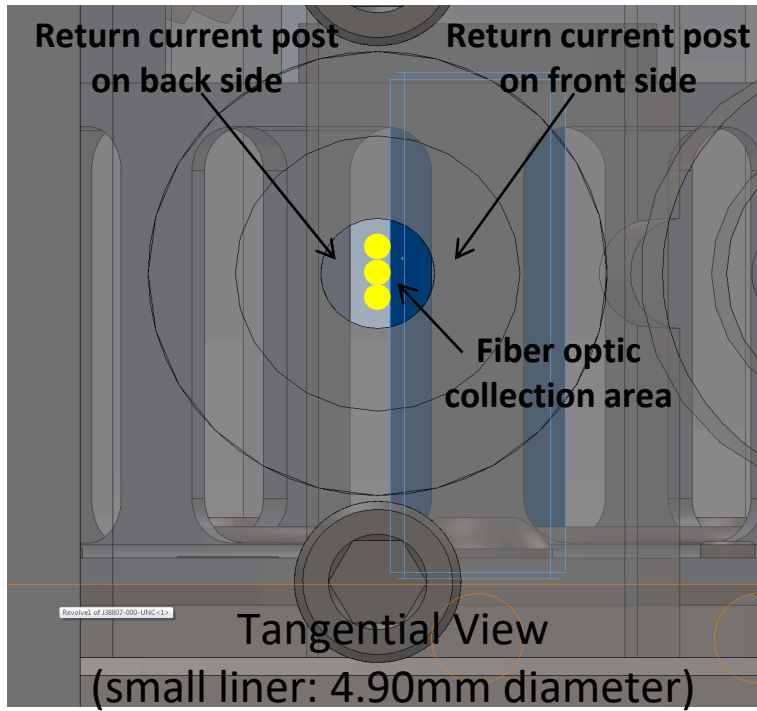
Fused Silica Window-no dopants
Grating: 150g/mm
Center Wavelength: 595nm
Sweep: 500ns
Combs: 35MHz (28ns)



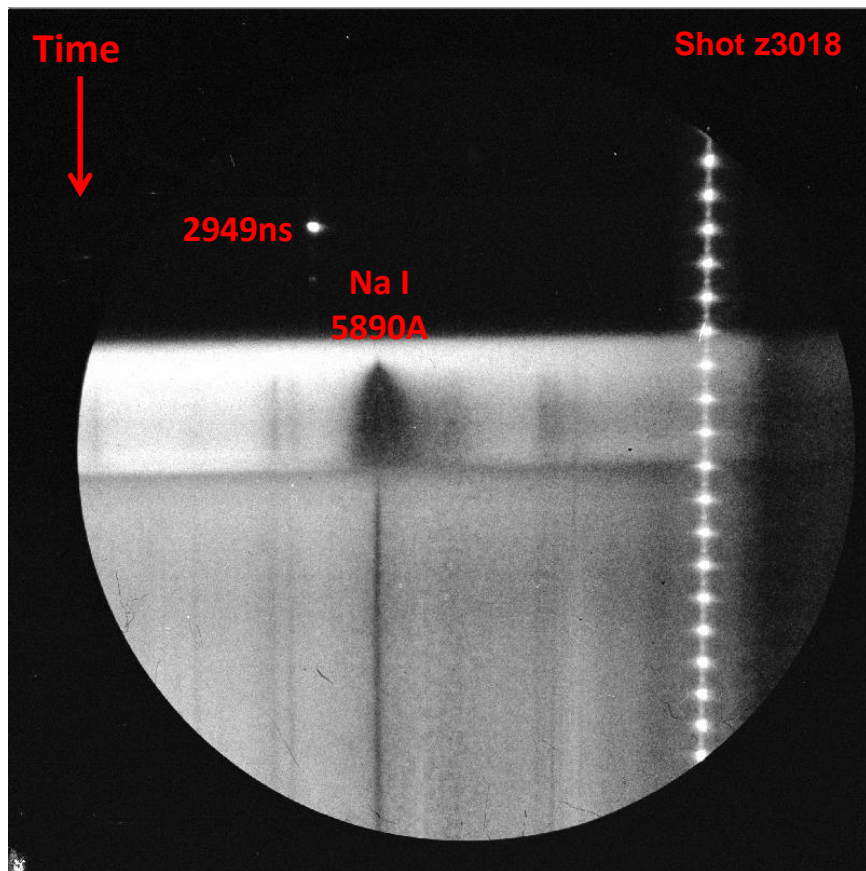
MgF₂ coated optics
Lithium and Sodium Dopants

- Dopants observed from both the anode and cathode, as well as from the optics.
- Highly broadened lithium neutral lines along the anode.

Hardware for MagLIF Liner Experiments with Slotted Return Can



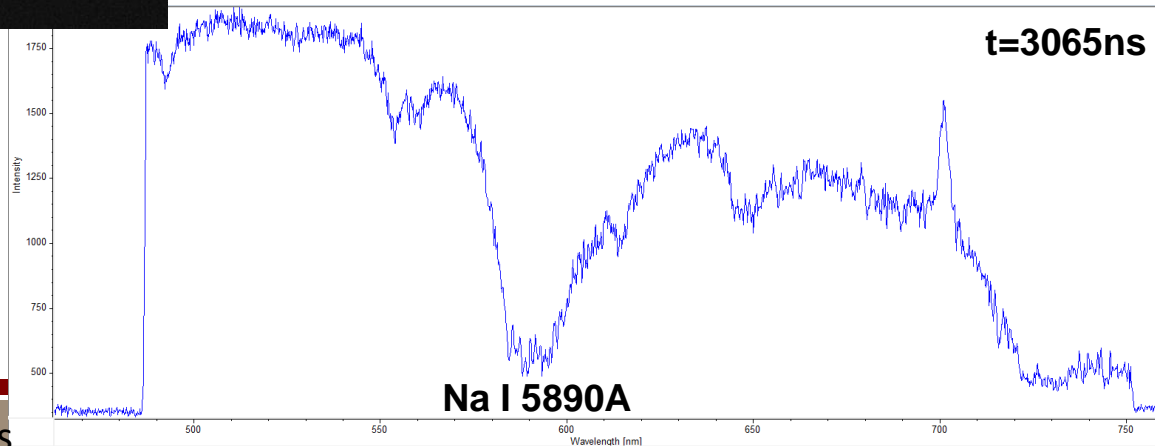
MagLIF Liner Experiments Show Sodium Line Broadening



Grating: 150g/mm
Center Wavelength: 618nm
Sweep: 480ns
Combs: 20nsec
Start of sweep: 2870ns
Impulse: 2949ns
Slit: 100 microns
Fiber: 100 microns
ND: 0.4 (40% transmission)
MCP Gain: 600V
LOS: 110
Green Laser: 5435A
Red Laser: 6328A

Experimental AR: 9
Uncoated Be Liner OD: 5.23mm

SVS1
Collimated beam, 1mm Aperture
7.5mm fl lens (uncoated)
Max counts: ~2000



*Film begins to saturate around 3500 counts

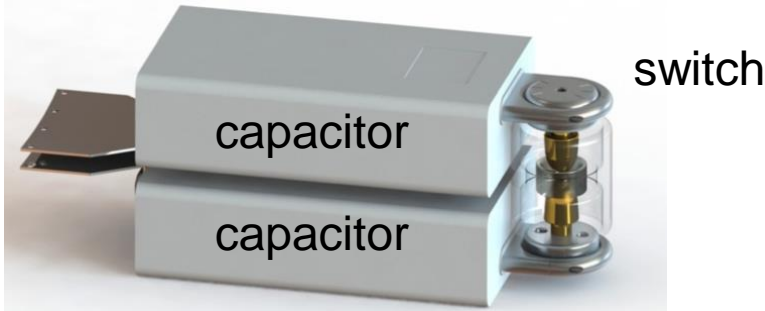
Summary and Conclusions

- Spectroscopic measurements of plasmas in the power flow regions on Z are ongoing.
- B-fields can be measured using the Zeeman effect, even when Stark and Doppler broadening is present, and for arbitrary B-field orientations, using techniques developed at the Weizmann Institute.
- Measurements of the magnetic field provide information regarding local current distributions, including current loss mechanisms.
- Techniques are being developed at the Weizmann Institute to analyze spectral data, taking into account opacities, impurities, signal to noise, and continua.
- Spectral measurements are needed to increase the fundamental physical understanding of plasmas and fields in high power machines.
- Present and future understanding and design of high power diodes relies heavily on kinetic PIC and hybrid (PIC/fluid) simulation models (ex. LSP and EMPHASIS). Experimental measurements are necessary to validate these models, and for accurate prediction of the performance of the next generation pulsed-power machines, such as Z-Next.

We are exploring a modular architecture that can scale to 300-1000 TW and is twice as electrically efficient as Z

Brick – “quantum” of the next gen systems
Single step pulse compression to 100 ns

Cavity – multiple bricks in parallel

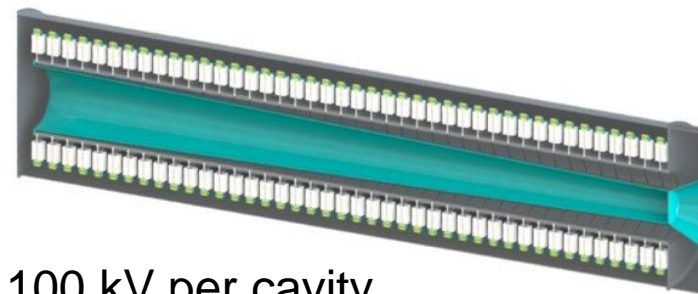
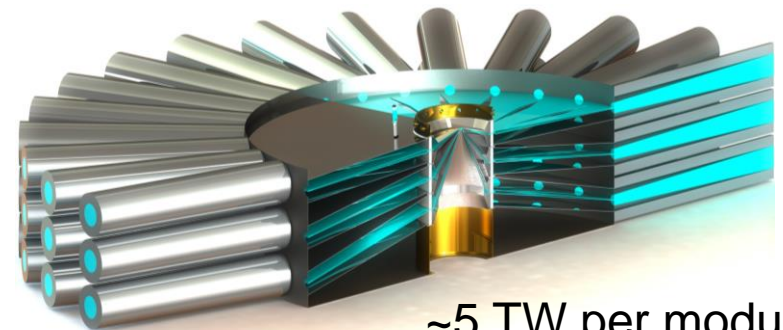


5.2 GW/800 J per brick

Module – multiple cavities in series

Machine – multiple modules and levels in parallel

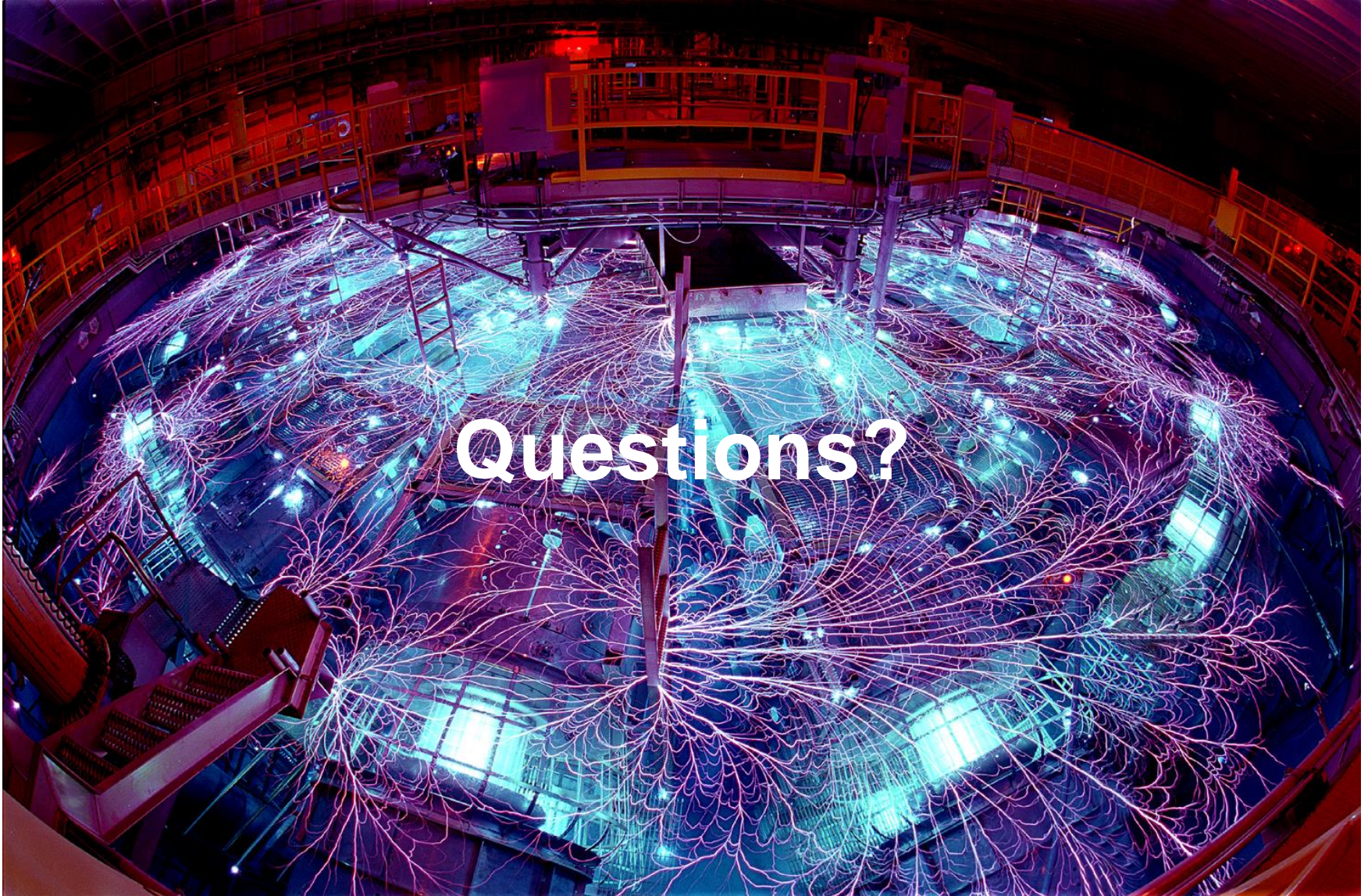
Linear Transformer Driver (LTD)



Next-gen machines: 20,000-200,000 bricks, 33-60 cavities/module, and 65-800 modules

- Continue to develop advanced techniques of spectral analyses, which include effects due to opacities, impurities, signal to noise, line emission, absorption, continua, and shielding.
- Determine plasma parameters such as species, ionization states, densities, and temperatures.
- Measure magnetic fields and currents in the A-K gap on Z. This will require greater signal to noise and/or plasma injection scheme (active dopants) [14].
- Implement a gated spectroscopy system at high resolution to record the spatial distribution of plasma on a single shot.
- Explore Stark shifts to measure E-fields as a function of time and space.
- Extend spectroscopic methods to other power flow regions.

Need scientists and engineers interested in pulsed-power and plasma physics to continue this work.



Extra Slides

Spectroscopy Diagnostics Overview

- **Visible Spectroscopy (400-700nm)**
 - Higher-level transitions of carbon, hydrogen, and oxygen, for measuring T_e and plasma composition
 - Ground state transitions of dopants (ex. NaI, MgI)
 - Doppler-shift measurements for velocities.
 - Zeeman splitting up to 300T
 - Stark broadening measurements for density determination
 - Stark shift, E-field measurements (ex. Li I 6708 A)
 - Ease of operation (optical fibers and/or standard optics)

- **UV Spectroscopy (200-400nm)**
 - Stronger line emission (ex. C III 2297 A)
 - Less continuum emission
 - Less stark broadening
 - Doppler broadening measurements
 - Fiber absorption issues
 - Fused silica (SiO_2) optics

- **Vacuum UV spectroscopy (50-200nm normal incidence grating)**
 - System needs to be in vacuum
 - Zeeman splitting at fields $> 300\text{T}$
 - Determination of plasma composition, T_e , and velocities
 - Ground state transitions of carbon, oxygen, and hydrogen
 - Special optics (MgF_2 , CaF_2) and detectors (no fibers)

